Free Form Fabrication of Ceramics By Stereolithography

Contract Number N00014-93-1-0302

Office of Naval Research

ONR Scientific Officer: Steven G. Fishman
01 January 1993- December 31, 1994

Final Technical Report
August 25, 1997

Principal Investigator: John W. Halloran
Department of Materials Science and Engineering
University of Michigan
Ann Arbor, MI 48109-2136

Free Form Fabrication of Ceramics by Stereolithography
Final Technical Report

Abstract

During this grant we showed that stereolithography can directly fabricate ceramic green bodies from ultraviolet (UV) curable solutions which contain dispersed ceramic powders. We demonstrated SLA of silica, a model refractory for metal casting molds, and SLA of alumina, which is promising for structural ceramics. Viscosity control for these highly concentrated suspensions and cure depth behavior were the main issues for fabricating a ceramic using stereolithography techniques. These ceramic SLA suspensions were evaluated in a stereolithography machine, and three-dimensional parts were built. Part building parameters, D_p and E_c, were determined for this suspension. Layer adhesion and subsequent processing resulted in good ceramic parts.

ONR Contract Information is summarized below
Contract Title: Free Form Fabrication of Ceramics by Stereolithography
Performing Organization: University of Michigan
Principal Investigator: John W. Halloran
Contract Number: N00014-93-1-0302 thru 12/31/94
R & T Project Number: cer9300---01
ONR Scientific Officer: Steven G. Fishman
Total Contract Value: $126,258
Contract Start Date: 1 January, 1993
Contract End Date: December 31, 1994

A. Scientific Research Goals

We were to develop a method for free form fabrication of ceramic green bodies using stereolithography of fluid suspensions of ceramic powders in photopolymerizable monomer solutions. With this method, ceramic objects are built with existing commercial stereolithography hardware and software, to allow ceramic prototypes to be made on these machines without modifications. This was successful.

B. Significant results in the past year

During this grant we showed that stereolithography can directly fabricate ceramic green bodies from ultraviolet (UV)

curable solutions which contain dispersed ceramic powders. We demonstrated SLA of silica, a model refractory for metal casting molds, and SLA of alumina, which is promising for structural ceramics. Viscosity control for these highly concentrated suspensions and cure depth behavior were the main issues for fabricating a ceramic using stereolithography techniques. These ceramic SLA suspensions were evaluated in a stereolithography machine, and three-dimensional parts were built. Part building parameters, D_p and E_c, were determined for this suspension. Layer adhesion and subsequent processing resulted in good ceramic parts.

Accurate objects are readily fabricated by stereolithography [SLA] from several choices of polymeric materials. We developed methods to expand the menu of materials to include ceramic materials for use as structural ceramics or for metal casting molds. Our method involves dispersing ceramic powders within an ultraviolet-curable solution. The suspension is used in the vat of an SLA machine as a "ceramic resin". The UV cured polymer acts as the binder to hold the ceramic particles together before firing. During firing, the polymer is removed and the ceramic powder is sintered, resulting in a ceramic part. In this paper we discuss the SLA properties of silica "resins" and alumina "resins", based on two UV-curable solutions.

To fabricate a quality ceramic, the suspension must contain a high ceramic solids content, about 50 v/o. These concentrated suspensions can be very viscous, especially when sinterable submicron ceramic powders are used. The suspension must be reasonably fluid and self-leveling [no yield stress]. The starting viscosity of the UV-curable solution is also very important. We have explored two UV-curable media: a very fluid aqueous solution and a relatively low viscosity diacrylate. To keep the viscosity low enough, the suspensions must be colloidally stabilized to a high degree with appropriate dispersants tailored for the particular powder surface chemistry and solution.

The critical SLA parameters cure depth [C_d] and energy density [E] are related to the resin properties D_p[penetration depth] and E_c [critical exposure] through the Beer-Lambert equation:

$$C_d = D_p \ln\left[\frac{E}{E_c}\right]$$

These same relations are obeyed for "ceramic resins". However concentrated suspensions are very turbid, and the cure depth is

limited by scattering of the UV radiation, rather than by adsorption. We find that the penetration depth for concentrated suspensions can be related to the properties of the resin by:

$$D_p \propto \beta \frac{d}{\phi} \frac{1}{\Delta n^2}$$

The penetration depth is controlled by the particle size (d), is inversely proportional to the volume fraction (ϕ) of ceramic and strongly dependent upon refractive index difference between the ceramic and the UV-curable solution, Δn. The term β is not yet well understood, but seems to involve the interparticle spacing and the UV wavelength. In most cases, a layer thickness of 200 microns or more could be achieved for the ceramic suspensions. Values for stereolithography parameters and early results for freeform fabrication of silica green bodies will be presented.

We used a silica powder as a model material for investment casting refractories, and an alumina as a typical sinterable powder with a submicron size. Several aqueous UV-curable solutions were prepared to determine the influence of refractive index on cure depth. The aqueous solution consisted of acrylamide and methylene bisacrylamide monomers in a aqueous solvent mixture. The diacrylate has the highest refractive index, 1.457, and therefore the smallest Δn between the ceramic and the UV-curable solution.

To prepare a high solids ceramic suspension, the monomers and solvents are mixed in a shear mixer. Ceramic powder and dispersants are added incrementally and the suspension is shear mixed between each increment until a solids loading of approximately 30 v/o is achieved. Further addition of ceramic and dispersants is followed by ball milling for complete homogenization and allow the dispersant(s) to stabilize the suspension. After the maximum solids loading is reached, 40-50 vol%, the photoinitiator(s) are added and the suspension is ball milled for several hours.

Initial testing of the cure properties were done with a conveyorized ultraviolet lamp apparatus. Note, the two strongest lines emitted by the lamp, 313 nm and 366 nm, correspond closely to the wavelengths used in SLA machines, 312 nm for the He-Cd laser and 351 nm for the Ar-ion laser. The exposure was determined by using a radiometer. After exposure, the polymerized sample was removed from the remaining uncured

suspension, and the cure depth was measured by optical or electron microscopy.

Promising ceramic suspensions were tested in a SLA-250 machine using an Ar-ion laser. The critical exposure (E_c) and penetration depth (D_p), were determined for each suspension with the "windowpanes" test geometry(6). Each pane in this part receives a different dose and the measured C_d versus dose was fit to Equation 1 to determine D_p and E_c. Cure depths with the Ar-ion laser were very close to cure depths with the UV lamp at the same energy density. After preliminary determination of D_p and E_c, several three-dimensional parts were fabricated.

The attached preprints present the results of this work in detail, which will not be repeated here. The reprint "Freeform Fabrication of Ceramics via Stereolithography" (J. American Ceramic Soc. 79 [10} 2601-608 (1996) present data on viscosity and cure depth, and show green and sintered ceramic SLA objects. Further theory and data on cure depth and light scattering are discussed in the attached preprint "Scattering of ultraviolet radiation in turbide suspensions" (J. Appied Physics, 81 (6) 2538-46 (1997)).

Conclusions

Highly concentrated suspensions of ceramic powders in photopolymerizable solutions can be cured by UV lamps or UV laser. Cure depth is proportional to the logarithm of energy through a Beer-Lambert relation, with the depth of penetration limited by scattering of UV radiation. Depth of penetration is inversely proportional to ceramic volume fraction and to the square of the refractive index difference between the ceramic and the suspension medium. Multilayer parts have been built using a SLA-250 with an Ar-ion laser, with promising accurate parts with good interlayer adhesion. Improved support structure and draw styles should eliminate the curl problems at the beginning of the build.

These first ceramic objects demonstrate the feasibility of stereolithography for directly building green ceramic objects, both for sintered structural ceramic parts and for refractory ceramic shells and cores for metal casting.

This work resulted in a U.S. patent application "Stereolithography Resin for Rapid Prototyping of Ceramics and Metals", M.G. Griffith, J. W. Halloran, and T-M Chu, but in 1997 the Patent Office did not allow this patent.

Work after the 1993 Grant

Research on this topic continued until December 1996 under a successor program N00014-95-1-0527. With ARPA funding, we acquired a 3D Systems SLA 250/40 stereolithography apparatus. This was used by Allan Brady, who is finishing a PhD thesis at Michigan. As a result of Brady's research, the SLA is routinely used to build ceramics with good accuracy and outstanding shape capability. These SLA ceramic objects can be seen at the web site:
msewww.engin.umich.edu/People/Halloran/SL/ceramicsla.html

D. List of Publications/Reports/Presentations

1. Papers Published in Refereed Journals

M.L. Griffith and J. W. Halloran, "Free Form Fabrication of Ceramics via Stereolithography", J. American Ceramic Soc. **79** [10], p. 2601-2608, [1996]

M.L. Griffith and J. W. Halloran, "Scattering of Ultraviolet Radiation in Turbid Ceramic Suspensions", J. Applied Physics **81** [10] pp. 2538-46[1997]

2. Non-Refereed Publications and Published Technical Reports

M.L. Griffith and J. W. Halloran, "Stereolithography of Ceramics" p. 970-979, International SAMPE Technical Conference Series, Vol 27, (1995)

M. L. Griffith Tien-Min Chu, Warren Wagner, and J. W. Halloran, "Ceramic Stereolithography for Investment Casting and Biomedical Applications", p. 31-38 in*Solid Free Form Fabrication Proceedings* , H.L. Marcus, J.J. Beaman, J.W. Barlow, D.L. Bourell, and R.H. Crawford, editors, 1995 SFF Symposium, Austin Texas, August 7-9, 1995

M. L. Griffith and J. W. Halloran "Stereolithography of Ceramics", p. 25-29, *Proceedings of The Sixth International Conf. on Rapid Prototyping*, Dayton, OH, June 4, 1995

M. L. Griffith and J. W. Halloran, "Ultraviolet Curable Ceramic Suspensions for Stereolithography of Ceramics", p. 529-534 in *Non-Traditional Design and Layered Manufacturing*, edited D. Dutta, PED-Vol. 68-2, Manufacturing Science and Engineering Book No. G0939B, American Society of Mechanical Engineers, 1994

M. L. Griffith and J. W. Halloran, "Ultraviolet Curing of Highly Loaded Ceramic Suspensions for Stereolithography of Ceramics", p. 396-403 in*Solid Free Form Fabrication Proceedings* , H.L. Marcus, J.J. Beaman, J.W. Barlow, D.L. Bourell, and R.H. Crawford, editors, SFF Symposium, Austin Texas, August 8-10, 1994, [1994]

M.L. Griffith, "Stereolithography of Ceramics", Ph.D. Thesis, University of Michigan, [1995]

3. Presentations

97th Annual Meeting of the American Ceramic Society, Cincinnatti, May 2, 1995: M. L. Griffith and J. W. Halloran, "Stereolithography of Ceramics"

M. L. Griffith and J. W. Halloran "Stereolithography of Ceramics", p. 25-29, The Sixth International Conf. on Rapid Prototyping, Dayton, OH, June 4, 1995

Solid Free Form Fabrication Symposium, Austin Texas, August 8, 1994: M. L. Griffith and J. W. Halloran, "Ultraviolet Curing of Highly Loaded Ceramic Suspensions for Stereolithography of Ceramics"

M. L. Griffith and J. W. Halloran, "Stereolithography of Ceramics", paper SXVII-13-95, May 2, 1995, 97th Annual Meeting of the American Ceramic Society, Cincinnatti

T.M. Chu, J. W. Halloran and W. Wagner, "Ultraviolet Curing of Highly Loaded Hydroxyapatite Suspension", paper SI-8-95, May 1, 1995, 97th Annual Meeting of the American Ceramic Society, Cincinnatti,

H. Summary of Publications/Patents/Presentations/Honors/Participants (Number Only)

a.	Number of Papers Submitted to Refereed Journal but not yet published:		0
b.	Number of Papers Published in Refereed Journals:		2
c.	Number of Books or Chapters Submitted but not yet Published:		0
d.	Number of Books or Chapters Published:		0
e.	Number of Printed Technical Reports& Non-Refereed Papers:		5
f.	Number of Patents Filed (in 1994):		1
g.	Number of Patents Granted :		0
h.	Number of Invited Presentations at Workshops or Prof. Society Meetings:		1
i.	Number of Contributed Presentations at Workshops or Prof. Society Meetings:		5
j.	Honors/Awards/Prizes for Contract/Grant Employees		0
k.	Number of Graduate Students and Post-Docs Supported at least 25%		1
	Grad Students:	Total	1
		Female	1
		Minority	0
	Post Doc:	Total	0
		Female	0
		Minority	0

Appendix

This Appendix includes reprints or copies of four of the principal publications resulting from this research grant. These are:

M.L. Griffith and J. W. Halloran, "Free Form Fabrication of Ceramics via Stereolithography", J. American Ceramic Soc. **79** [10], p. 2601-2608, [1996]

M.L. Griffith and J. W. Halloran, "Scattering of Ultraviolet Radiation in Turbid Ceramic Suspensions", J. Applied Physics **81** [10] pp. 2538-46[1997]

M. L. Griffith Tien-Min Chu, Warren Wagner, and J. W. Halloran, "Ceramic Stereolithography for Investment Casting and Biomedical Applications", p. 31-38 in*Solid Free Form Fabrication Proceedings* , H.L. Marcus, J.J. Beaman, J.W. Barlow, D.L. Bourell, and R.H. Crawford, editors, 1995 SFF Symposium, Austin Texas, August 7-9, 1995

M. L. Griffith and J. W. Halloran "Stereolithography of Ceramics", p. 25-29, *Proceedings of The Sixth International Conf. on Rapid Prototyping*, Dayton, OH, June 4, 1995

journal

J. Am. Ceram. Soc., 79 [10] 2601–608 (1996)

Freeform Fabrication of Ceramics via Stereolithography

Michelle L. Griffith*,† and John W. Halloran*

Department of Materials Science and Engineering, The University of Michigan, Ann Arbor, Michigan 48109-2136

Ceramic green bodies can be created using stereolithography methods where a ceramic suspension consisting of 0.40–0.55 volume fraction ceramic powder is dispersed within an ultraviolet-curable solution. Three ceramic materials were investigated: silica for investment casting purposes, and alumina and silicon nitride for structural parts. After mixing the powders in the curable solution, the ceramic suspension is photocured, layer by layer, fabricating a three-dimensional ceramic green body. Subsequent binder removal results in a sintered ceramic part. Three-dimensional objects have been fabricated from a 0.50 volume fraction silica suspension.

I. Introduction

FREEFORM fabrication involves shaping without the use of molds or tooling and has been accomplished with ceramics by selective laser sintering[1] and three-dimensional printing[2] techniques. Stereolithography (SL) is currently the most popular method for freeform fabrication,[3,4] but SL has not been used to produce ceramics. Stereolithography creates a solid body by scanning a laser beam on a liquid monomer, curing it in a line-by-line, layer-by-layer sequence.[5] Stereolithography machines or apparatuses (SLA), such as the SLA-250 and SLA-500 (3D Systems, Valencia, CA) are widely used with photopolymerizable polymers, including acrylates and epoxies. We have extended the stereolithography method so it can be used for freeform fabrication of ceramics, including structural ceramics such as alumina or silicon nitride and refractories such as silica-based shells and cores for investment casting. This is done via ultraviolet (UV) curing of a highly concentrated suspension of ceramic particles in a photopolymerizable liquid. The UV-curable liquid creates the polymer binder to form a net shape ceramic green part without the need of molds. The green part can be given a conventional binder burnout and sintering treatment.

"Stereolithography," invented by Chuck Hull,[6] was one of the first freeform fabrication technologies. This technique involves the polymerization of liquid monomers from exposure to ultraviolet radiation from a laser.[7] Figure 1 shows a schematic of the apparatus. With a stereolithography machine, a three-dimensional (3D) part is fabricated in a layer-by-layer process. First, a 3D computer image is sliced into many cross-sectional layers 150–200 μm thick. Using the information of each slice, laser radiation is scanned on the surface of the liquid monomer to draw the layer. As the laser scans the surface, the monomer is photocured to a polymer, where the polymerization depth is controlled by the radiation exposure (mJ/cm^2) and set to the layer thickness. When the layer is finished, the support platform and first layer move downward into the vat of liquid monomer resin. The liquid monomer flows across the first polymerized layer, and to ensure the second layer of monomer is of the desired thickness, a recoat blade moves across the surface. The laser scans this new surface, polymerizing the second layer. This process is repeated many times until the part is finished. When part building is done, the platform is raised and the solid polymer part emerges from the vat.

A candidate ceramic stereolithography suspension must satisfy several requirements. Since a high-quality ceramic is the goal, the freeform ceramic green body must have a high density, either for its refractory properties or so it can be readily sinterable to form a dense ceramic. The SLA suspension, at a 0.50–0.65 solids volume fraction, is a highly concentrated suspension, which must have a relatively low viscosity, preferably with no pronounced yield point. To operate in an SLA resin tank, the ceramic SLA suspension must be at least as fluid as conventional SLA resins (viscosity less than 3000 mPa·s) for proper flow during recoat of the new layer.[8] Obtaining effective dispersion for submicrometer powders requires careful design of the colloidal dispersant system. The viscosity of the pure monomer resin is extremely important. A lower starting viscosity usually results in a lower final viscosity for the suspension. Thus suspensions were prepared in low-viscosity UV-curable liquids, and dispersants were carefully selected to control the colloidal chemistry, and therefore the rheology.

The stereolithography apparatus builds parts from layers 150–200 μm thick. It is necessary that the cure depth of these highly loaded suspensions be equal to or greater than 150–200 μm after exposure to ultraviolet radiation in order to fabricate a ceramic green body in a sufficient amount of time. This concentrated ceramic suspension must be sufficiently transparent to ultraviolet radiation to permit an acceptable depth of cure. Powder suspensions can have a very high turbidity due to radiation scattering, even if the ceramic itself is transparent to UV. The scattering-induced turbidity limits the distance of penetration of the UV radiation into the suspension, and largely determines the depth of cure, C_d, for a ceramic suspension. The depth of cure can be modeled by assuming it to be the depth at which the UV beam is attenuated from the incident intensity (E_0) down to the minimum intensity required to achieve photocuring (E_c) for the particular photoinitiator/monomer system. This can be derived from the Beer–Lambert law:[9]

$$C_d \propto \frac{d}{\phi}\frac{1}{Q}\ln\left[\frac{E_0}{E_c}\right] \quad (1)$$

where the cure depth is proportional to the average particle

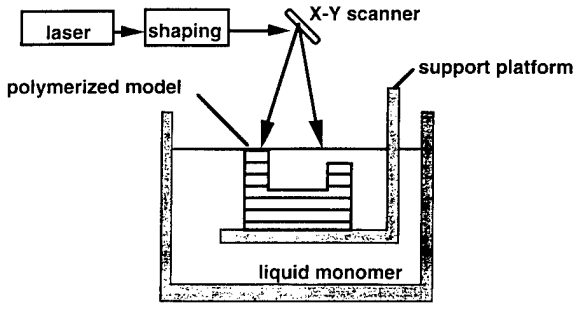

Fig. 1. Schematic of the 3D Systems' stereolithography apparatus (SLA) for fabrication of three-dimensional objects.

C. F. Zukoski—contributing editor

Manuscript No. 192329. Received September 11, 1995; approved March 28, 1996.
Supported by the Office of Naval Research under Grant No. N00014-913-1-0302.
*Member, American Ceramic Society.
†Now at Sandia National Laboratories, Albuquerque, New Mexico 87185.

Table I. Particle Size (d) and Refractive Index (n) for Ceramic Powders

Material	Density (g/mL)	d_{50} (μm)	d_{10} (μm)	d_{90} (μm)	Refractive index n at 366 nm
Silica†	2.65	2.29††	0.79	8.70	1.56
Silicon nitride‡	3.24	0.44‡‡	0.10	0.78	2.10
Alumina AKP-50§	3.96	0.46††	0.30	0.63	1.70
Alumina AKP-15§	3.96	0.61††	0.41	0.93	1.70
Alumina RC-HP¶	3.96	0.34‡‡	0.18	0.60	1.70

†α-quartz, Atlantic Equipment Engineering, Bergenfield, NJ. ‡UBE E10, UBE Industries, Tokyo, Japan. §AKP-15 and AKP-50 grades, Sumitomo Chemical, Tokyo, Japan. ¶RC-HP, Reynolds, from Malakoff Industries, Malakoff, TX. ††MICROTRAC particle size analyzer, Leeds & Northrop, North Wales, PA. ‡‡Particle size distribution analyzer, Model No. CAPA-700, Horiba, Irvine, CA.

size (d) and the logarithm of the exposure (E_0) and inversely proportional to the volume fraction ceramic (ϕ). The materials' scattering ability is described in the scattering efficiency term Q, where Q is a function of the refractive index difference between the ceramic and the UV-curable solution:

$$Q = \beta \Delta n^2 \tag{2}$$

Therefore, the cure depth is inversely proportional to $\Delta n^2 = (n_{ceramic} - n_{solution})^2$, where n is the refractive index. The term β is related to the particle size and the wavelength of the radiation, and this will be discussed later in the paper.

One important feature is the choice of the photoinitiator system. Photoinitiators react with the ultraviolet radiation and initiate polymerization. The absorptivity must be tuned to the particular UV wavelength and the concentration maximized for efficient photopolymerization through the depth of the suspension.[10]

The most important part of the SLA ceramic suspension is the ability to fabricate three-dimensional ceramic objects. Issues including shape integrity and adhesion between layers will be discussed.

II. Experimental Procedure

(1) Characteristics of the Ceramic Powders

Three ceramic materials were investigated in this research. Table I shows the particle size, density, and refractive index of the powders. Silica was chosen as a model material for investment casting applications. As is typical with investment casting refractory materials, the particle size was large and had a broad particle size distribution to improve the packing density. This silica powder was a milled quartz with a median particle size of 2.3 μm. The silicon nitride was a diimide-derived powder with a median particle size of 0.44 μm. Several alumina powders were used, including a high-purity ball-milled Bayer alumina (0.34 μm median, Reynolds' RC-HP) and two precipitated aluminas (0.46 and 0.61 μm, Sumitomo AKP-50 and AKP-15).

Table I also includes the refractive index information for silica,[11] silicon nitride,[11] and alumina.[12] The absorption edges are far below 313–370 nm UV wavelength range, so these three materials should be transparent to the UV radiation.

(2) Photopolymerizable Solutions

A photopolymerizable solution contains two or more materials. The minimum two materials are monomer(s) and photoinitiator(s). Nonreactive solvents may be added to reduce the viscosity, since most of the photomonomers have high viscosities, on the order of tens to thousands of mPa·s. Curing a monomer-solvent system creates a gel, which should have less polymerization shrinkage and easier binder removal upon firing.

The cured resin is the final product for conventional stereolithography, so cured resin properties are critical. For ceramic stereolithography, the photopolymer is only a binder for the ceramic particles in the green body, and the cured resin does not have to be very strong to impart adequate strength to the green ceramic. The polymer will later be removed, so its concentration should be minimized.

Two formulations of UV-curable solutions were examined: an aqueous acrylamide-based solution and a nonaqueous diacrylate. The aqueous acrylamide solution was a 9:1 mixture of acrylamide and methylenebisacrylamide in 0.50–0.70 volume fraction water, similar to a "gelcasting" formulation,[13,14] with the thermal initiators replaced with photoinitiators. This solution was further modified to vary the refractive index. Table II shows the refractive indices of the aqueous solutions, which were varied over the range 1.38–1.44 using mixtures of water (n = 1.33) and ethylene glycol (n = 1.43). The refractive index was measured by Abbey refractometry (Valentine Precision model, Industro Scientific, North Merrick, NY). The nonaqueous diacrylate is based upon the common monomer hexane diol diacrylate [HDDA], which is the 1–6 hexamethylene ester of acrylic acid (2-propenoic acid). The refractive index of the diacrylate is shown in Table II. This diacrylate is more viscous (6–12 mPa·s) than the aqueous media (1 mPa·s), but has a higher refractive index, and offers a good compromise between reactivity and low viscosity. It is similar to the usual acrylic ester-based monomers used in conventional stereolithography. Acrylate polymers are commonly used as ceramic binders.

(3) Preparing the Concentrated Ceramic Suspension

To prepare the suspensions, the UV-curable solution was prepared first, without the photoinitiators, and the ceramic powder (plus dispersants) was added incrementally. Up to about 0.30–0.35 solids loading, the suspension was mixed and homogenized in a high speed shear mixer. Above 0.35 volume fraction ceramic, more time was required for the dispersants to adsorb and colloidally stabilize the suspension, so ball milling was preferred for mixing and homogenization. When the maximum solids loading had been reached, the photoinitiators were added, and the suspension was ball-milled for 5 h to thoroughly mix the photoinitiators.

(4) Ultraviolet Curing of the Ceramic Suspensions

The curing behavior of the suspensions was first tested in a simple lamp apparatus (Hanovia UV Laboratory System, Hanovia, NJ). The ultraviolet curing apparatus consists of an ozone-free low-pressure mercury UV lamp enclosed in a housing with a conveyor belt to carry the samples under the lamp for exposure. The exposure dose of UV radiation was controlled with the conveyor speed and lamp setting, and measured with a radiometer (IL390B, International Light, Newburyport, NJ). The two main intensities of this UV lamp (313 and 366 nm) correspond to the laser intensities for the two SLA models

Table II. Refractive Index (n) and Viscosity for the Ultraviolet-Curable Solutions

Ultraviolet-curable solution	Refractive index (n)	Viscosity (mPa·s)†
Aqueous 1	1.382	~1
Aqueous 2	1.399	~1
Aqueous 3	1.415	~1
Aqueous 4	1.418	~1
Aqueous 5	1.441	~1
Diacrylate, HDDA	1.457	6

†Shear rate = 3 s^{-1}.

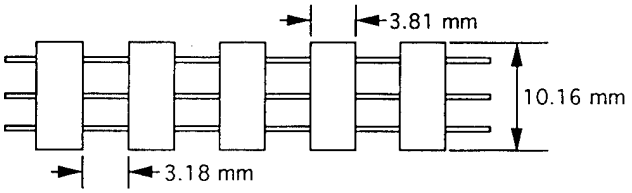

Fig. 2. Windowpane geometry showing five individual panes. Each pane receives a different exposure dose resulting in a different cure depth.

(313 nm for the He–Cd and 351 nm for the Ar ion). For the same exposure (mJ/cm^2), the lamp and laser produced similar cure depths.

A 2–3 mm thick layer of ceramic suspension in a petrie dish was passed through the apparatus and exposed to 100–5200 mJ/cm^2 ultraviolet radiation over a period of 2–10 s. After exposure, the polymerized layer was lifted off of the uncured suspension and rinsed. The cure depth was measured on the dried film by either optical or scanning electron microscopy.

Promising ceramic suspensions, with low viscosities and large cure depths, were tested in a stereolithography apparatus, Model SLA-250 with an Ar-ion laser (351 nm). For all ceramic suspensions, the first experiment was to fabricate "windowpanes" test parts,[15] illustrated in Fig. 2, to test for shape integrity. The laser scans the surface of the suspension to draw the three horizontal lines, followed by the outline of the "panes." Next the laser scans the interior of each pane at different scanning velocities so that each pane receives a different dose. After fabrication of the windowpanes, the cured part was removed from the rest of the uncured suspension and rinsed in either deionized water for the aqueous suspensions or ethanol for the acrylate suspension. Each windowpane thickness was measured with a micrometer to obtain the cure depth.

For three-dimensional parts, the stereolithography file 'Box' was used to fabricate a ceramic green body. Figure 3 shows the object, a hollow 2.54 cm (1 in.) cubed box with a 45° angle cut into one side. Before the box is fabricated, a support structure or scaffold is fabricated for easy removal of the 3D object from the support platform. The scaffold was designed by Bridgeworks (Solid Concepts, Valencia, CA) software.

III. Results and Discussion

(1) Viscosity of the Concentrated Ceramic Suspensions

All ceramic powders were easy to disperse in the aqueous UV-curable solutions. The colloidal chemistry is better understood for aqueous suspensions,[16–20] whether acidic (silica) or basic (alumina, silicon nitride) powders are chosen. Figure 4 shows the viscosity versus solids loading for silica dispersed in the lowest refractive index aqueous solution (aqueous 1).

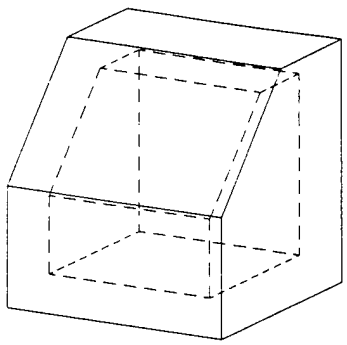

Fig. 3. Line drawing of the stereolithography file "box." The hollow box is 2.54 cm (1 in.) cube, with 3.2 mm (1/8 in.) wall thickness, and a 45° angle cut into one side.

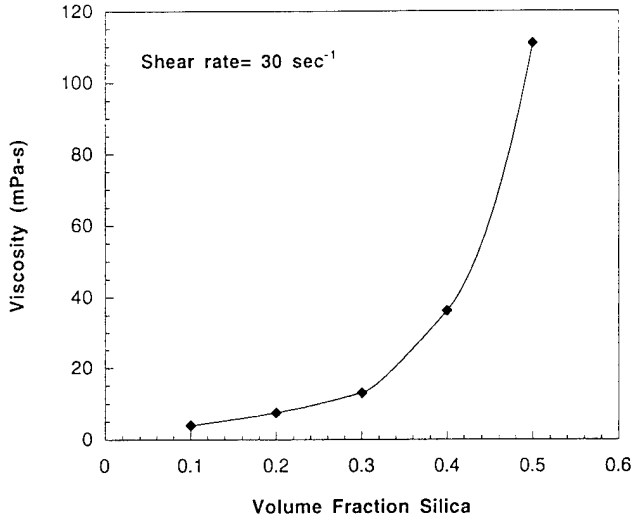

Fig. 4. Viscosity versus volume fraction silica added to aqueous solution 1 with $n = 1.382$.

As expected, the viscosity increases as the solids loading increases;[21] however, the suspension's viscosity at 0.50 solids loading is 120 mPa·s for a shear rate of 30 s^{-1}. This is well below the upper limit of 3000 mPa·s.

All suspensions are shear thinning, as shown in Fig. 5 for 50 vol% silica dispersed in two aqueous solutions (Nos. 1 and 4). The effective yield stresses for the aqueous suspensions are quite low, about 185 mPa, thereby promoting correct layer recoating. Table III shows the suspensions studied, the maximum solids loading, and the low shear rate viscosity of the ceramic suspensions.

The acrylate suspensions were exceedingly viscous, with viscosities greater than 3000 mPa·s for low shear rates at solids loadings less than 0.30. It is much more difficult to disperse ceramics in nonaqueous solutions,[22] but a 0.40 alumina solids loading in HDDA was achieved with a viscosity of 3000 mPa·s (shear rate = 6 s^{-1}).

(2) Ultraviolet Curing of Concentrated Ceramic Suspensions

For fabrication of ceramic green bodies via stereolithography to be feasible, the minimum cure depth per layer must be approximately 200 μm. Many users of the stereolithography apparatus cure polymer layers of 150 μm; this allows for smoother surfaces and finer features to be fabricated.

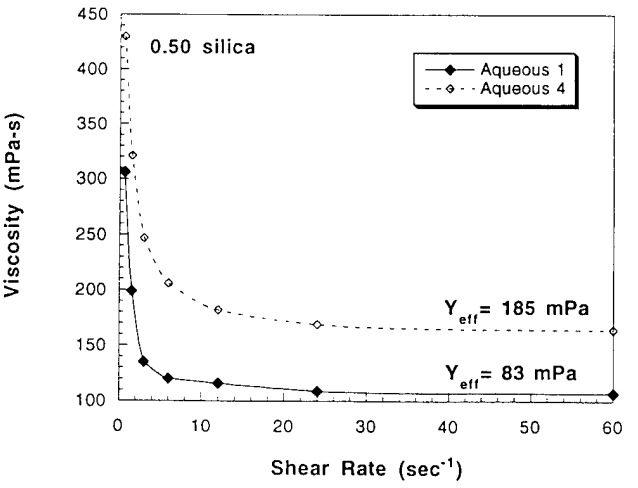

Fig. 5. Viscosity versus shear rate for 0.50 solids loading silica in two aqueous solutions, Aqueous 1 ($n = 1.382$) and Aqueous 4 ($n = 1.418$). Both suspensions have low yield point, Y_{eff}, values.

Table III. Maximum Solids Loading for Ceramic Suspensions and Corresponding Viscosities

Maximum solids ceramic	Ultraviolet-curable solution	Viscosity (mPa·s)*
0.50 silica (d = 2.29 μm)	All aqueous (n = 1.382–1.441)	200–500
0.50 alumina (d = 0.46 and 0.61 μm)	Aqueous 1 (n = 1.382)	500
0.40 alumina (d = 0.34 μm)	HDDA (n = 1.457)	3000

*Shear rate = 3 s^{-1}.

(A) Silica: Of the three materials, the cure depth of the silica suspensions should be the largest since silica has the smallest refractive index (n = 1.56). Figure 6 shows the cure depth versus inverse volume fraction silica added to the aqueous solution with a refractive index of 1.3824 (No. 1). As expected from the Beer–Lambert law and Eq. (1), the cure depth decreases as more silica is added to the suspension. At 0.50 solids loading of silica, the cure depth is greater than the minimum requirement, where C_d = 360 μm at an exposure dose of 1500 mJ/cm^2. Even at 0.55 volume fraction, the cure depth is above 200 μm, where C_d = 330 μm.

The cure depth is reasonable for 0.50 solids loading silica dispersed in the lowest refractive index solution, but a larger value would allow the SLA operator to choose the layer thickness. Figure 7 shows the cure depth versus dose for 0.50 solids loading of silica dispersed in a variety of aqueous UV-curable solutions. As the refractive index difference decreases from Δn^2 = 0.0317 to 0.0142, the cure depth increases from 250 to 700 μm for a dose of 1500 mJ/cm^2. A small change in refractive index for the UV-curable solution (4%) results in a 3-fold increase in the cure depth. Note, the cure depth versus the log of the exposure shows linear behavior as predicted from Eq. (1).

In stereolithography the dose is usually less than 500 mJ/cm^2. These low doses cannot be achieved with the lamp apparatus, and therefore it was necessary to study the cure depth behavior at low doses in an SLA. Figure 8 shows the cure behavior for two ceramic suspensions: 0.50 solids loading of silica added to an aqueous solution (n = 1.418) and 0.40 solids loading of alumina added to the diacrylate. At large doses, the cure depth is nearly the same as the lamp results for the silica suspension. Therefore, the lamp accurately models the cure behavior for these concentrated suspensions.

In Fig. 8, there are different regions of cure depth behavior. At doses above 300 mJ/cm^2, the cure behavior is linear and similar to the lamp results. For the silica suspension at doses lower than 300 mJ/cm^2, the cure depth has linear behavior, but with a different slope. For very low doses, less than 80 mJ/cm^2, the cure depth is most likely arrested by oxygen inhibition.[23] For the middle dose region, 80–300 mJ/cm^2, the cure behavior is more likely in an anaerobic condition,[24] where the polymerization rate strongly affects the cure depth as well as radiation scattering by the ceramic particles. At large doses, $E_0 > 300$ mJ/cm^2, the cure behavior is dominated by the scattering effects of the ceramic particles, whereas the photoinitiation rate saturates, producing enough free radicals for the polymerization

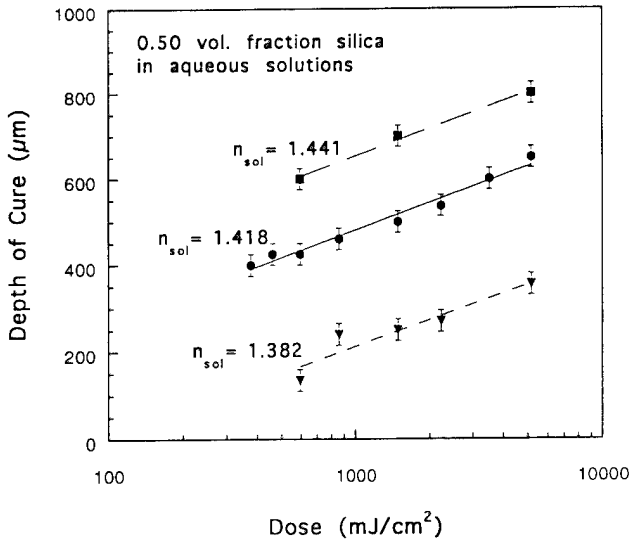

Fig. 7. Cure depth versus exposure dose for 0.50 volume fraction silica dispersed in three aqueous UV-curable solutions.

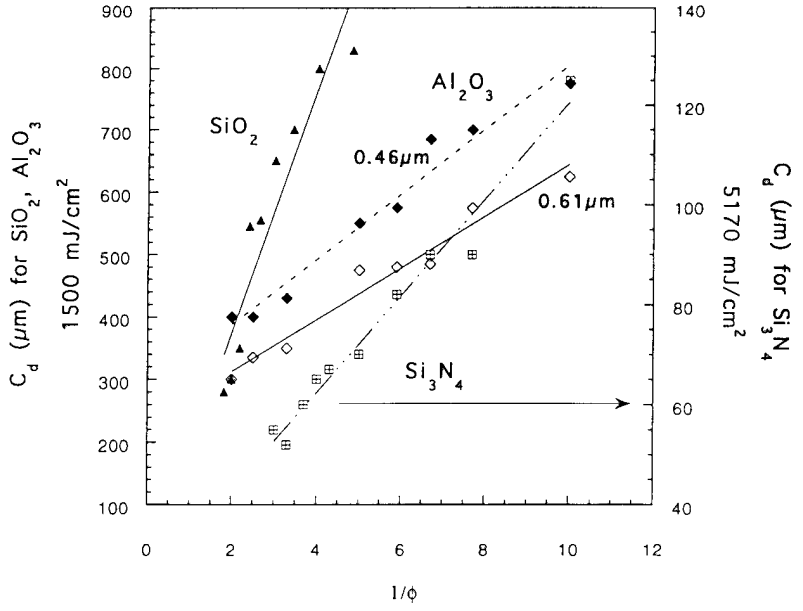

Fig. 6. Cure depth (C_d) versus volume fraction (1/1ϕ) for three ceramic suspensions, where all curves exhibit linear behavior. The silica and alumina powders are dispersed in the aqueous solution with a refractive index of 1.382 and the silicon nitride powder dispersed in the diacrylate.

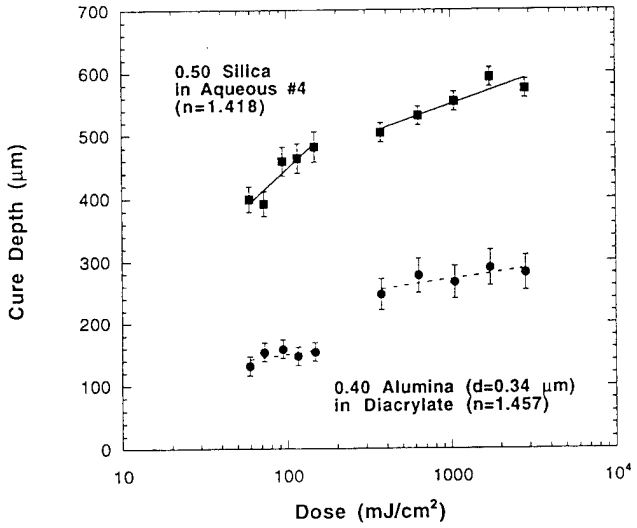

Fig. 8. Cure depth behavior over a wide exposure dose range for silica and alumina suspensions cured in stereolithography apparatus.

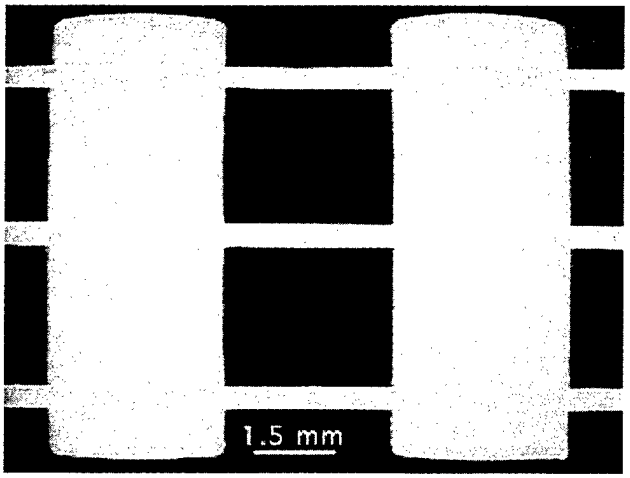

Fig. 9. Two representative panes built on SLA-250 with Ar-ion laser. Panes were fabricated from 0.40 volume fraction alumina (d = 0.34 μm) in the diacrylate.

reaction, and is a secondary effect on the cure depth. The important point is the cure depth at doses as low as 50 mJ/cm^2 is still greater than 200 μm.

The alumina–diacrylate suspension shows a pronounced change in cure depth for doses less than 300 mJ/cm^2, similar to the silica–aqueous suspension. Oxygen inhibition most likely affects the low dose behavior for diacrylate solutions.[25,26]

(B) Alumina: Different grades of alumina were used in the UV-curable solutions to determine the effect of particle size on the cure depth. Figure 6 shows the cure depth versus inverse volume fraction alumina (two grades) added to the low refractive index aqueous solution (No. 1). At 0.50 solids loading and a dose of 1500 mJ/cm^2, both suspensions have cure depths greater than 200 μm. The smaller particle size alumina had a larger cure depth, 400 versus 300 μm. Table IV shows the results for different grades of alumina dispersed in a variety of aqueous UV-curable solutions, and particle size effects will be discussed later in this paper.

Windowpanes were fabricated from a 0.40 volume fraction alumina in the diacrylate solution. Figure 9 shows two representative panes from the windowpane. Note the spatial integrity with accurate laser lines and rectangular sections. The experimental panes are larger than the expected dimensions due to more side scattering in turbid suspensions. This error (5–15%) could be easily compensated for in the laser scanning pattern. Figure 8 shows the cure depth behavior for this suspension, where the necessary cure depth is achievable for doses larger than 300 mJ/cm^2. The green alumina windowpanes were slowly heated to 600°C to remove the polymers and then fired at 1550°C to sinter the alumina. Figure 10 shows the resulting microstructure of fully dense alumina.

Another requirement for stereolithography of ceramics is the layers must not be evident after firing of the green body. Figure 11(a) shows a sintered two-layer alumina part. The 0.40 volume fraction alumina in diacrylate suspension was tape cast with a thickness of 100 μm. The first layer was cured, and then another 100 μm was tape cast and cured. The alumina green body was sintered, and Figs. 11(a) and (b) show the fracture

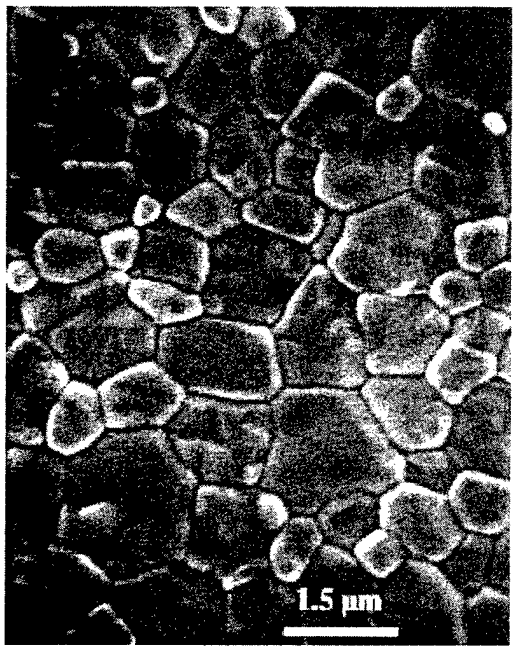

Fig. 10. Sintered alumina windowpane showing fully dense microstructure with grain sizes between 1 and 2 μm.

surface of the two-layer alumina part. The interface of the layer is not visible as shown in Fig. 11(b).

(C) Silicon Nitride: Silicon nitride has a high refractive index, n = 2.1, which resulted in poor cure depths when dispersed in the aqueous UV-curable solution. At 0.10 solids loading in the solution with n = 1.382, the cure depth was only 21 μm, and the cure depth decreased to 10 μm at a 0.20 solids loading. Even though a fluid 0.50 volume fraction silicon nitride suspension was achievable, the system was not studied further because of the low cure depth behavior.

Table IV. Cure Depth for 0.50 Solids Loading Alumina Dispersed in Aqueous UV-Curable Solutions

Alumina	Ultraviolet-curable aqueous solution	Cure depth (μm)	
		1500 mJ/cm^2	5170 mJ/cm^2
AKP-50 (d = 0.46 μm)	Aqueous 1 (n = 1.382)	400 ± 25	
AKP-15 (d = 0.61 μm)	Aqueous 1 (n = 1.382)	300 ± 25	400 ± 30
Reynolds (d = 0.34 μm)	Aqueous 4 (n = 1.418)	450 ± 30	600 ± 30

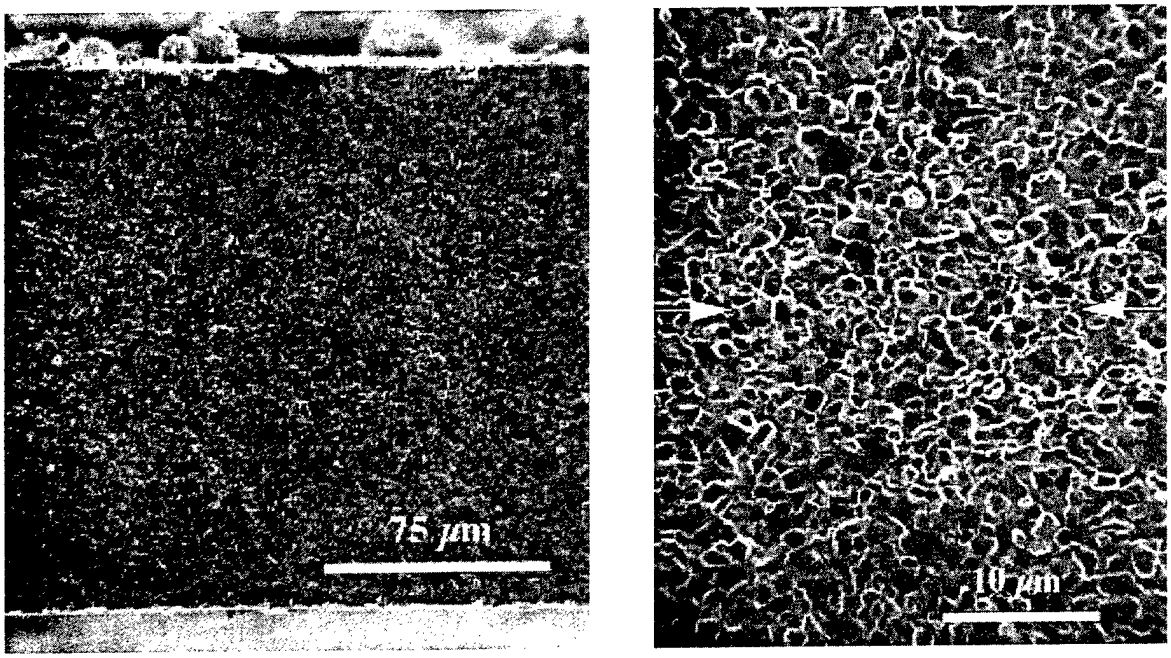

Fig. 11. (a) Low-magnification micrograph of fracture surface for sintered two-layer alumina part. (b) High-magnification micrograph showing the interface of the individual layers which cannot be resolved.

Figure 6 shows the cure depth versus inverse solids loading in the diacrylate, where $\Delta n^2 = 0.413$, a 11% decrease from the aqueous suspension. At 0.30 solids loading, the cure depth was 60 μm, an improvement over the aqueous suspension but well below the necessary 200 μm.

(3) SLA Silica Parts

For the fabrication of the first ceramic green body using stereolithography, 0.50 volume fraction silica was dispersed in the aqueous solution with $n = 1.418$ (see Fig. 7). Figure 12 shows the first silica box fabricated by stereolithography. This 136-layer box was built in about 4 h, where each layer was 150 μm thick. Because of time requirements, the box was started 0.635 cm (1/4 in.) from the bottom of the design; therefore, in the z-direction the box should be 1.905 cm (3/4 in.) tall. Note, the sides and the 45° angle were built accurately, where the x and y dimensions were 2.545 cm (1.002 in.) each. This represents an error of 50 μm, which can easily be compensated for during the laser scanning sequence.

Figure 13 shows a side view of the two silica boxes fabricated on the SLA-250. At the beginning of build, the layers curled because of polymerization shrinkage. This is most likely due to the laser draw style[27] where the polymerization shrinkage and curl behavior can be minimized by the choice of scanning sequence or space filling routine. The simple draw style chosen for the first attempt promoted curl in the beginning of the build which was evident until the 20th layer, after which the cured body was sufficiently rigid so the new polymerizing layer cannot cause further distortion. Subsequent research will determine the correct scanning sequence (SLA work performed over a 3 day period at 3D Systems in Valencia, CA).

The box tops are slightly rounded because the recoat blade was not used during the fabrication of the parts (modified resin vat for small suspension volume). After a layer was cured, the support platform was lowered into the fluid suspension, and the new layer flowed on top of the cured layer. Time was allowed for the suspension to equilibrate, creating a smooth layer ready

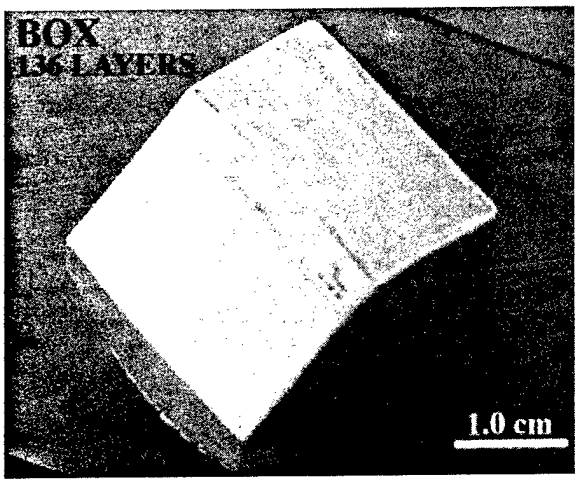

Fig. 12. First stereolithography part built using Michigan ceramic stereolithography suspension. Ceramic green body is 0.50 volume fraction silica cured in aqueous gel ($n = 1.418$). Box consists of 136 layers, each 150 μm thick.

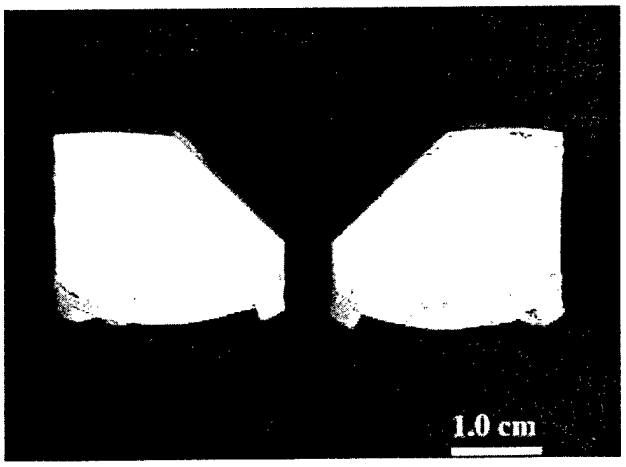

Fig. 13. Side view of two silica boxes built on SLA. Curl behavior is apparent at the beginning of build due to scanning style of the laser, whereas the slightly rounded tops are due to no recoat step during fabrication. The sides and 45° angles were accurately built.

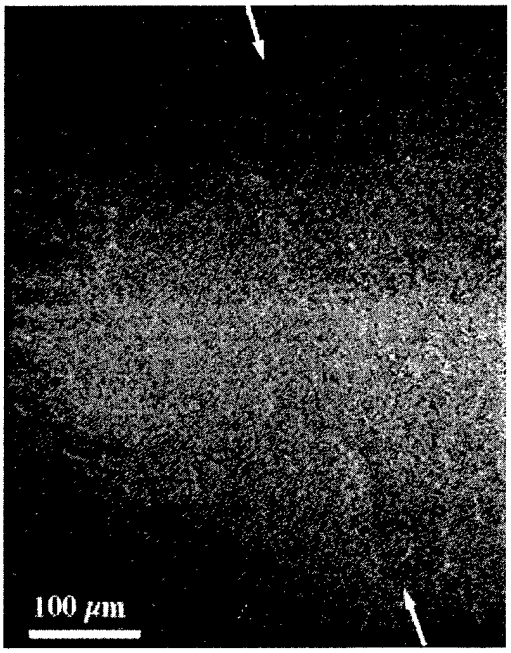

Fig. 14. Micrograph of silica box exterior, showing "knitting" of three layers. The arrows represent the interface of two layers, where the layers are not distinguishable.

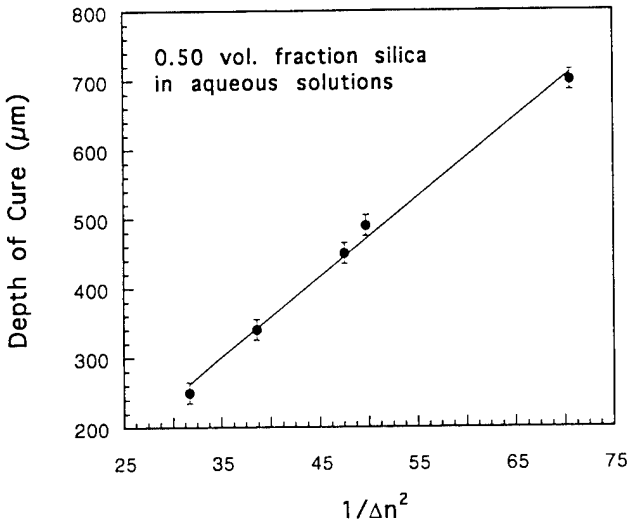

Fig. 15. Cure depth versus refractive index difference for 0.50 volume fraction silica dispersed in five aqueous UV-curable solutions.

for exposure. A time of 45 s was insufficient for the layers of the box top to equilize to a flat layer.

Figure 14 shows the adhesion between the individual layers for the silica box. Arrows point to a possible layer interface, but the interface is barely distinguishable. Note, in the picture there should be three layer interfaces which are not visible. Therefore, there is no problem with knitting the layers in the photopolymerization of a highly concentrated ceramic suspensions.

(4) Theory

The curing behavior of ceramic suspension can be modeled with Eqs. (1) and (2), which are derived and discussed in detail elsewhere.[9] Three linear relationships are expected for highly concentrated suspensions which scatter radiation. First, the cure depth should be linearly proportional to the logarithm of the exposure dose, and previous figures (Figs. 7 and 8) show this behavior. Note, for the SLA curves, only the large exposure dose regions are considered because this is the scattering limited region. Secondly, the cure depth should be inversely proportional to the volume fraction solid, $1/\phi$. Figure 6 shows C_d vs $1/\phi$ for a variety of ceramic suspensions, for silica and two alumina powders in the aqueous acrylamide solution, and silicon nitride in the diacrylate. All the data have a reasonably linear fit. Although we could not prepare a fluid 0.50 volume fraction silicon nitride suspension in the diacrylate, we can predict that the cure depth at this volume fraction should be $C_d = 40$ μm. Thirdly, cure depth should be inversely proportional to the square of the refractive index difference, Δn^2. Figure 15 shows the cure depth of 0.50 volume fraction silica in five aqueous solutions as a function of the inverse of the refractive index difference, $1/\Delta n^2$, demonstrating a good linear fit.

Particle size should play an important role, since it is well known that the particle size influences the scattering of the radiation.[28,29] The behavior of highly concentrated suspensions is not well understood. Figure 6 showed the cure depth increased for the smaller particle size alumina. We have not been able to reconcile this with simple scattering theories, such as Rayleigh-Gans or Mie theory, which relate the scattering to particle size for very dilute suspensions. For these highly concentrated suspensions, however, we find empirically that it is the ratio of the interparticle spacing (S) to the wavelength of the radiation (λ) that influences the cure depth, where $\beta = S/\lambda$. The scattering equation (Eq. (1)) using $Q = (S/\lambda)(\Delta n^2)$, accurately predicts the magnitude of the cure depth for these concentrated ceramic suspensions. Full details describing the theory and prediction of cure behavior for concentrated ceramic suspensions are described elsewhere.[9]

IV. Conclusions

Freeform fabrication of ceramics can be done with stereolithography using concentrated suspensions of powder in photopolymerizable media. Aqueous acrylamide-based suspensions have been demonstrated for alumina and for silica with viscosities below 500 mPa·s and cure depths above 300 μm at a dose of 1500 mJ/cm^2. These are adequate for useful fabrication by stereolithography. An acrylamide suspension of silicon nitride was fluid, but had insufficient depth of cure. Nonaqueous diacrylate-based suspensions have higher cure depths, but higher viscosities.

The first ceramic stereolithography part was built from a 0.50 volume fraction silica suspension in the aqueous acrylamide system using an SLA-250 with an Ar ion laser. This part was a box-shaped component with 136 layers, each 150 μm thick. Interlayer adhesion was adequate. Stereolithography test parts from alumina in the diacrylate system readily sintered to full density at 1550°C. Interlayer boundaries could not be distinguished in the sintered alumina.

Depth of cure can be modeled with a modified Beer–Lambert law, assuming scattering to be the primary mechanism. Cure depth is proportional to the logarithm of dose, inversely proportional to volume fraction ceramic, and inversely proportional to the square of the refractive index difference between the ceramic powder and the medium.

Acknowledgments: We wish to thank Dr. Paul Jacobs, Dr. Thomas Pang, and Kelly Kwo, at 3D Systems, for their time and use of their stereolithography apparatus.

References

[1]U. Lakshminarayan, S. Ogrydiziak, and H. L. Marcus, "Selective Laser Sintering of Ceramic Materials"; pp. 16–26 in Proceedings of the Solid Free Form Fabrication Symposium (Austin, TX, August 1990). Edited by H. L. Marcus *et al.* University of Texas, Austin, TX, 1990.

[2]M. J. Cima and E. M. Sachs, "Three Dimensional Printing: Form, Materials, and Performance"; pp. 187–94 in Proceedings of the Solid Free Form Fabrication Symposium (Austin, TX, August 1991). Edited by H. L. Marcus *et al.* University of Texas, Austin, TX, 1991.

[3]P. F. Jacobs, "Stereolithography 1993: Epoxy Resins, Improved Accuracy, and Investment Casting"; pp. 249–62 in Proceedings of the Fourth International Conference on Rapid Prototyping (Dayton, OH, June 1993). Edited by R. Chartoff *et al.* University of Dayton, Dayton, OH, 1993.

[4]M. Burns, *Automated Fabrication: Improving Productivity in Manufacturing*; pp. 40–43, 49–53. Prentice Hall, Englewood Cliffs, NJ, 1993.

[5]P. F. Jacobs, *Rapid Prototyping and Manufacturing: Fundamentals of Stereolithography*; pp. 1–23. Society of Manufacturing Engineers, Dearborn, MI, 1992.

[6]C. Hull, "Apparatus for Production of Three-Dimensional Objects by Stereolithography," U.S. Pat. No. 4 575 330, 1986.

[7]P. F. Jacobs, *Rapid Prototyping and Manufacturing: Fundamentals of Stereolithography*; pp. 11–18. Society of Manufacturing Engineers, Dearborn, MI, 1992.

[8]Dr. Paul Jacobs, Director of Research and Development, 3D Systems, Valencia, CA; private communication.

[9]M. Griffith; Ph.D. Thesis, Ch. 6. University of Michigan, Ann Arbor, MI, March 1995.

[10]S. P. Pappas, "Radiation Curing—A Personal Perspective"; pp. 1–20 in *Radiation Curing: Science and Technology*. Edited by S. P. Pappas. Plenum Publishing, New York, 1992.

[11]E. D. Pawlik, *Handbook of Optical Constants of Solids*; pp. 749–64, 771–74. Harcourt Brace Jovanovich, New York, 1985.

[12]C. L. Haertling, S. Yoshikawa, and R. R. Newnham, "Thick Film Patterned Ceramics Using UV-curable Pastes," *J. Am. Ceram. Soc.*, **73** [11] 3330–44 (1990).

[13]A. C. Young, O. O. Omatete, M. A. Janney, and P. A. Menchofer, "Gelcasting of Alumina," *J. Am. Ceram. Soc.*, **74** [13] 612–18 (1991).

[14]O. O. Omatete, M. A. Janney, and R. A. Strehlow, "Gelcasting—A New Ceramic Forming Process," *Am. Ceram. Soc. Bull.*, **70** [10] 1641–49 (1991).

[15]P. F. Jacobs, *Rapid Prototyping and Manufacturing: Fundamentals of Stereolithography*; pp. 27–281. Society of Manufacturing Engineers, Dearborn, MI, 1992.

[16]D. Meyers, "Colloids and Colloidal Stability"; p. 187–220 in *Surfaces, Interfaces, and Colloids*. VCH Publishing, New York, 1990.

[17]R. J. Hunter, *Foundations of Colloid Science*; pp. 329–447. Clarendon Press, Oxford, England, 1986.

[18]M. J. Crimp, R. E. Johnson, J. W. Halloran, and D. L. Feke, "Colloidal Behavior of SiC and Si_3N_4"; pp. 539–49 in *Science of Ceramic Chemical Processing*. Edited by L. L. Hench and D. R. Ulrich. Wiley, New York, 1986.

[19]S. G. Malghan, "Dispersion of Si_3N_4 Powders: Surface Chemical Interactions in Aqueous Media," *J. Colloid Surf.*, **62**, 87–99 (1992).

[20]F. H. Baader, T. J. Graule, and L. J. Gaukler, "Rheology of Concentrated Aqueous Alumina Suspensions"; to be published in the Proceedings of the 8th CIMTECH–World Ceramic Congress and Forum on New Materials (Florence, Italy, June 1994).

[21]Th. Tadros, "Rheology of Highly Concentrated Suspensions"; pp. 71–87 in *Advances in Fine Particle Processing*. Edited by J. Hanna and Y. A. Attia. Elsevier Science Publishers, New York, 1990.

[22]F. M. Fowkes, "Dispersions of Ceramic Powders in Organic Media"; pp. 411–21 in Advances in Ceramics, Vol. 21, *Ceramic Powder Science*. Edited by G. L. Messing, K. S. Mazdiyasni, J. W. McCauley, and R. A. Haber. American Ceramic Society, Westerville, OH, 1987.

[23]J. P. Foussier, "An Introduction to the Basic Principles in UV Curing"; pp. 49–117 in *Radiation Curing in Polymer Science and Technology*, Vol. I. Edited by J. P. Foussier and J. F. Rabek. Elsevier Applied Science, London, England, 1993.

[24]Dr. Douglas Neckers, Bowling Green State University, Photochemistry Department; private communication.

[25]J. P. Foussier, "Excited-State Reactivity in Radiacal Polymerisation Photoinitiators"; pp. 1–61 in *Radiation Curing in Polymer Science and Technology*. Vol. II. Edited by J. P. Foussier and J. F. Rabek. Elsevier Applied Science, London, England, 1993.

[26]C. Decker and K. Moussa, "UV-Radiation and Laser-Induced Polymerization of Acrylic Monomers"; pp. 439–56 in ACS Symposium Series, No. 417, *Radiation Curing of Polymeric Materials*, Proceedings of the American Chemical Society. American Chemical Society, Washington, DC, 1990.

[27]S. Ulett, R. P. Chartoff, A. J. Lightman, J. P. Murphy, and J. Li, "Reducing Warpage in Stereolithography through Novel Draw Styles"; pp. 242–89 in Proceedings of the Solid Free Form Fabrication Symposium (Austin, TX, August 1994). Edited by H. L. Marcus *et al.* University of Texas, Austin, TX, 1994.

[28]H. C. van de Hulst, *Light Scattering by Small Particles*. Wiley, New York, 1957.

[29]P. W. Barber and S. C. Hill, *Light Scattering by Particles: Computational Methods*. World Scientific Publishing, Teaneck, NJ, 1990. □

Scattering of ultraviolet radiation in turbid suspensions

Michelle L. Griffith[a] and John W. Halloran
Materials Science and Engineering Department, The University of Michigan, Ann Arbor, Michigan 48109-2136

(Received 2 November 1995; accepted for publication 10 December 1996)

A Beer's law expression for the penetration depth of ultraviolet radiation in a concentrated suspension of scattering particles is used to model the depth of cure for a suspension of ceramic particles in a medium of photocurable monomers. The cure depth is predominantly controlled by the square of the refractive index difference between the ceramic particles and the medium, $\Delta n^2 = (n_p - n_0)^2$. A secondary effect on the cure depth is the ratio of the interparticle spacing to the ultraviolet wavelength. Theoretical results agree with experimental data for 0.40–0.50 volume fraction ceramic-filled suspensions. © *1997 American Institute of Physics.* [S0021-8979(97)06506-7]

I. INTRODUCTION

The interaction between radiation and particles has been investigated for a variety of phenomena including the scattering of visible light resulting in blue skies and red sunsets.[1] For particles that are much smaller than the radiation wavelength, scattering behavior is governed by the polarizability tensor,[2] and particles of simple shape that are much larger than the wavelength may be treated by a combination of geometric optics and Fraunhofer diffraction.[3] Complex theoretical models are needed to solve the problem for particles of intermediate size.[4] We consider here the penetration of ultraviolet (UV) radiation in a very concentrated suspension (containing up to 0.50 volume fraction particles) for which no simple expressions are available.[2] Our particular interest is the case where the particle diameter is similar to the radiation wavelength ($d \propto \lambda$). For this case, scattering theories describe the interaction of a single object, usually a sphere, suspended in a medium[5] and cannot be simply applied to concentrated suspensions. For example, the multi-particle scattering equations of Mie[6,7] are limited to very dilute suspensions (less than 0.10 solids loading particles), so Mie theory does not accurately describe multiparticle interactions for highly filled suspensions.

It would be advantageous to have a simple expression to describe this radiation interaction. This is particularly relevant for photopolymerization of concentrated suspensions of ceramic powders, which has been used for freeform fabrication of ceramics by stereolithography techniques.[8–11] Stereolithography produces very accurate three dimensional polymer parts[12–14] by photopolymerization of a liquid resin with a computer-controlled UV laser. The plastic object is built from a sequence of thin layers about 200 μm thick. The depth of cure, D_c, or the resin polymerized by the UV laser radiation is a critical parameter. A conventional resin is an absorbing medium, and the attenuation of the UV energy with depth can be accurately modeled with Beer's law:

$$E = E_0 \exp(-\gamma L)$$

relating energy density (E) to depth (L) through the extinction coefficient (γ). The cure depth (D_c) is the distance required to attenuate E to the minimum energy density (E_{crit}) required for photopolymerization or gellation of the resin, so the cure depth can be described by

$$D_c = [1/\gamma] \ln(E_0/E_{crit}).$$

Thus the extinction coefficient links cure depth to laser intensity and scan speed and is a vital parameter for stereolithography.

The polymerization depth is reduced by dispersing ceramic powders in a UV-curable medium. For ceramic volume fractions above about 0.10, the cure depth is controlled by the scattering of the UV radiation. It will be shown that the cure depth of turbid ceramic suspensions can be modeled accurately with an equation of the form:

$$D_c = \frac{2\langle d \rangle}{3\tilde{Q}} \frac{n_0^2}{\Delta n^2} \ln\left(\frac{E_0}{E_{crit}}\right),$$

where $\langle d \rangle$ is the average particle size, Δn^2 is the square of the refractive index difference between the ceramic and the medium [$\Delta n^2 = (n_p - n_0)^2$], ϕ the volume fraction solids, E_0 the energy density, and $\tilde{Q}$ is the scattering efficiency term. This equation is a Beer's law expression with an effective extinction coefficient, $\gamma_{eff} = 3\tilde{Q}\Delta n^2/2\langle d \rangle n_0^2$.

This article will cover the general aspects of scattering in relation to particle characteristics, medium characteristics, and regions where scattering or absorption dominate. Theoretical results will be compared to experimental data for highly concentrated ceramic suspensions.

II. EXPERIMENT

Details of the experimental work are discussed elsewhere.[15,16] This article contains the necessary information related to understanding the photopolymerization behavior of highly concentrated ceramic suspensions.

A. Ceramic suspensions

Ceramic suspensions were made by dispersing ceramic powders in UV-curable solutions. Three ceramic materials were investigated:

[a]Present address: Sandia National Laboratories, P.O. Box 5800, MS 0958, Albuquerque, NM 87185; Electronic mail: mlgriff@sandia.gov

 0021-8979/97/81(6)/2538/9/$10.00

TABLE I. Particle size (d), density, and refractive index (n) for ceramic powders.

Ceramic	Density (g/cm^3)	50th percentile particle size $\langle d \rangle$ (μm)	10th percentile particle size d_{10} (μm)	90th percentile particle size d_{90} (μm)	Refractive index, n_p
Silica[a]	2.65	2.29[e]	0.79	8.70	1.56
Silicon nitride[b]	3.24	0.44[f]	0.10	0.78	2.10
Alumina[c] AKP-50	3.96	0.46[e]	0.30	0.63	1.70
Alumina[c] AKP-15	3.96	0.61[e]	0.41	0.93	1.70
Alumina[d] RC-HP	3.96	0.34[f]	0.18	0.60	1.70

[a]α-quartz, Atlantic Equipment Engineering, Bergenfield, NJ.
[b]UBE E10, UBE Industries, Tokyo, Japan.
[c]AKP-15 and AKP-50 grades, Sumitomo Chemical, Tokyo, Japan.
[d]Reynolds RC-HP, Malakoff Industries, Malakoff, TX.
[e]MICROTRAC particle size analyzer, Leeds & Northrop, North Wales, PA.
[f]Particle size distribution analyzer, Model #CAPA-700, Horiba, Irvine, CA.

(1) silica, a low refractive index ceramic for investment casting applications,
(2) alumina, with a medium refractive index for structural ceramics, and
(3) silicon nitride, a high refractive index material also used for structural ceramic applications.

Table I shows the particle size, density, and refractive index for these ceramic powders.[17,18]

Two varieties of UV-curable solutions were prepared:

(1) aqueous solutions using acrylamide monomers, similar to the "gel casting" formulation[19,20] with the thermal initiators replaced by photoinitiators, and
(2) a low viscosity diacrylate monomer, hexane diol diacrylate, similar to existing monomer resins used in stereolithography.

Table II shows the refractive index values for the constituents and for the different UV-curable solutions (measured by Abbey refractometry). It was possible to vary the refractive index of the aqueous solutions by the addition of ethylene glycol as a solvent.

For photopolymerization to occur, small amounts of photoinitiators, less than 2.0 wt %, were added to the UV-curable solution. The photoinitiators were matched to the long ultraviolet wavelengths ($\lambda > 300$ nm), and the concentration chosen for the maximum depth of cure.[21] After preparing the UV-curable solution, ceramic powder was added, incrementally, and mixed in a high shear mixer. After reaching the maximum solids loading, the photoinitiators were added and the suspension mixed for approximately 5 h to ensure complete homogenization.

TABLE II. Refractive indices for UV-curable solutions and the basic constituents.

Basic materials for UV-curable solution	Refractive index, n	UV-curable solution	Refractive index, n_0
acrylamide	1.53	Aqueous 1	1.38
methylene bisacrylamide	1.52	Aqueous 2	1.40
ethylene glycol	1.43	Aqueous 3	1.41
water	1.33	Aqueous 4	1.42
		Aqueous 5	1.44
		Diacrylate	1.46

B. Ultraviolet exposure

Each suspension was exposed to ultraviolet radiation from either a mercury lamp or a laser. The two strongest lines emitted by the lamp, 313 and 366 nm, correspond closely to the wavelengths used in stereolithography machines, 312 nm for He–Cd and 351 nm for Ar–ion laser. Cure depths were similar whether exposed to the lamp or the laser.[16] Exposure doses (mJ/cm^2) were measured using a radiometer. After exposure, the polymerized ceramic film was removed from the remaining material, rinsed, and the cure depth was measured either by optical or electron microscopy.

C. Experimental results

1. Concentration dependence

Figures 1(a) and 1(b) show the concentration dependence on the cure depth for silica, alumina, and silicon nitride dispersed in a variety of UV-curable solutions. At 0.50 solids loading for the silica and alumina suspensions, the cure depth is greater than 200 μm, thereby satisfying the requirements for use in stereolithography.

The cure depth, D_c, is plotted against the inverse of volume fraction solids, $1/\phi$, showing linear behavior. Even though a 0.50 volume fraction silicon nitride/diacrylate suspension was not prepared, the cure depth is predicted to equal 40 μm. The largest cure depths are for the silica suspensions, for which the square of the refractive index difference, Δn^2, has the smallest value. However, at 0.50 solids loading, the cure depth for the alumina and silica suspensions are similar.

2. Dose dependence

Figures 2(a) and 2(b) show the dose dependence for 0.50 solids loading ceramic suspensions. As expected, the cure depth is larger as the dose increases, following Beer's law and the cure depth equation, D_c. Note that the cure depth

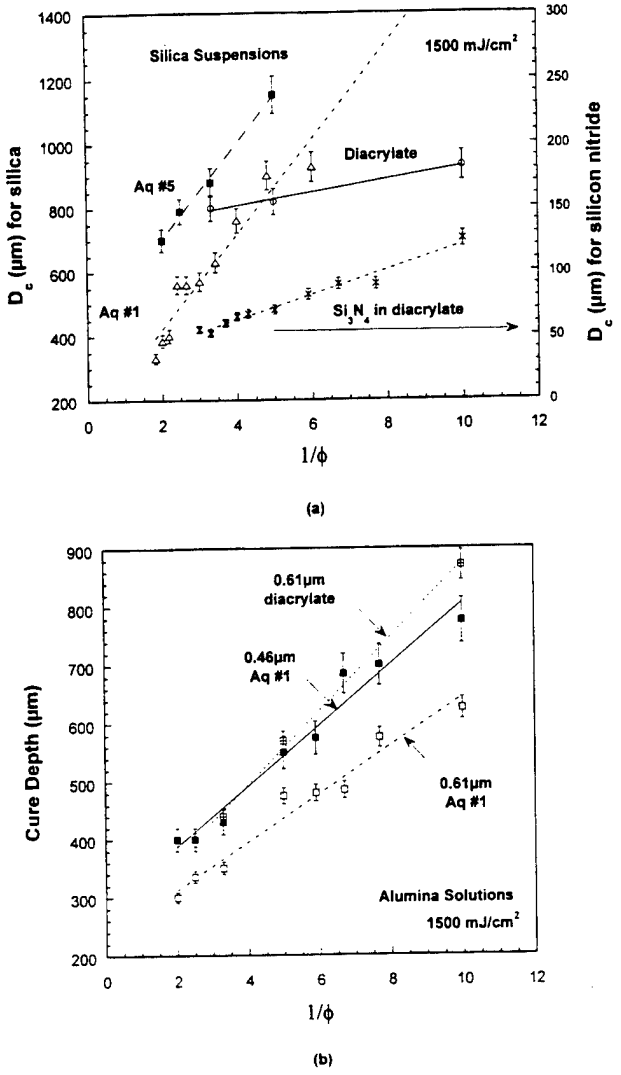

FIG. 1. (a) Depth of cure (D_c) vs inverse volume fraction ($1/\phi$) for three silica suspensions and for silicon nitride dispersed in diacrylate. All samples received an exposure dose of 1500 mJ/cm^2. (b) Depth of cure (D_c) vs inverse volume fraction ($1/\phi$) for three alumina suspensions. All suspensions received an exposure dose of 1500 mJ/cm^2.

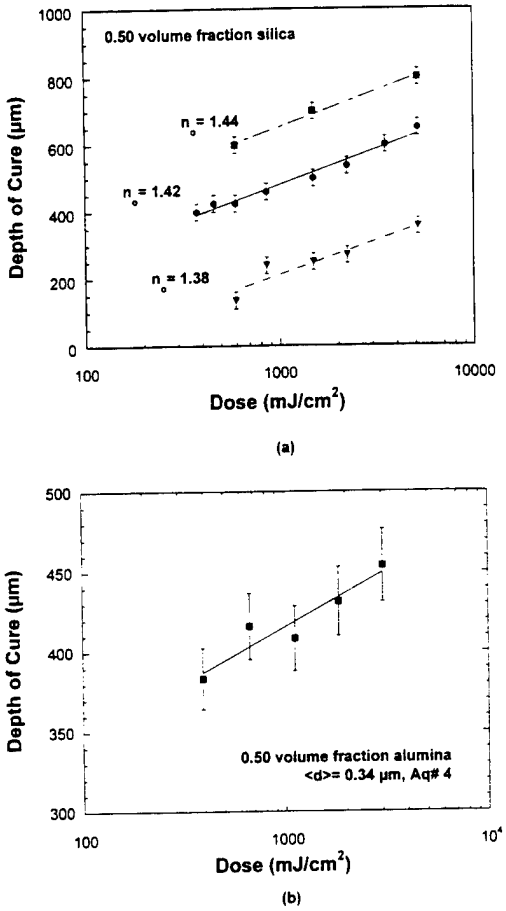

FIG. 2. Depth of cure (μm) vs dose (mJ/cm^2) for 0.50 volume fraction silica in three aqueous UV-curable solutions. (b) Depth of cure (μm) vs dose (mJ/cm^2) for 0.50 volume fraction alumina dispersed in aqueou.. solution #4.

greatly increases as the square of the difference in the refractive index between silica and the aqueous UV-curable solution is reduced. At 1500 mJ/cm^2, the cure depth changes from 250 to 700 μm as Δn^2 changes from 0.032 to 0.014.

3. Particle size dependence

Figure 1(b) shows the cure depth versus $1/\phi$ for different particle size alumina powders dispersed in a variety of UV-curable solutions. All suspensions have a linear fit, following the expected cure depth behavior. However, the smaller particle size alumina has a larger cure depth in the aqueous solution which is contradictory to the expectation that $D_c \propto d$.

III. THE SCATTERING EQUATION D_c

Scattering theory is based upon an electromagnetic wave impinging on a single particle, with a particular refractive index and size, in a medium with a different refractive index.[2,5] Most theories assume that the medium does not absorb the radiation, and for turbid suspensions the scattering properties will dominate the penetration depth.

For multi-particle scattering, a form of Beer's law is utilized where the particles act as separate scattering centers and the scattering term is a summation of the individual scattering centers. For the summation to be valid, the distance between particles must be greater than two radii which corresponds to suspensions at solid loadings of less than 0.10 when using particles on the order of 1 μm. However, there are spaces between particles which are roughly one particle radius, and therefore the summation form for multi-particle scattering will be used without much loss in validity. The general form of Beer's law is

$$E = E_0 \exp(-\gamma L), \tag{1}$$

where E_0 is the energy density (measured in mJ/cm^2) of the radiation at the surface of suspension, γ is the extinction coefficient or turbidity term, and L is the path length the radiation travels.

Two processes occur as the UV radiation travels into the highly concentrated suspension. First, and predominantly, the particles scatter the radiation. Second, the UV-curable solution absorbs part of the radiation, thereby reducing its intensity. The radiation which is not absorbed travels further into the suspension and the two processes continue until the energy of the radiation reaches a critical limit, E_{crit}, in which

the remaining radiation is absorbed by the monomer resin. This minimum energy is required for gellation of the monomer. One can describe the polymerization depth for a turbid ceramic suspension, where the path length equals the depth of cure, $L \rightarrow D_c$, and the exposure equals a critical exposure, $E \rightarrow E_{crit}$, where

$$E_{crit} = E_0 \exp(-\gamma D_c), \quad \text{or} \quad D_c = \gamma^{-1} \ln\left(\frac{E_0}{E_{crit}}\right).$$

The extinction coefficient can be described by[22]

$$\gamma = \frac{3}{2}\frac{\phi Q}{\langle d \rangle},$$

where $\langle d \rangle$ is the average particle diameter, ϕ is the volume fraction particles, and Q is the extinction coefficient efficiency.

After substitution, the scattering equation becomes

$$D_c = \frac{2\langle d \rangle}{3Q}\frac{1}{\phi}\ln\left[\frac{E_0}{E_{crit}}\right]. \tag{2}$$

Equation 2 exhibits three linear proportional relationships expected for highly turbid suspensions:

(1) the cure depth versus $1/Q$ at fixed volume fraction and $\langle d \rangle$,
(2) the cure depth versus $1/\phi$ at fixed Q and $\langle d \rangle$, and
(3) the cure depth versus $\ln(E_0)$ at fixed ϕ, $\langle d \rangle$, and Q. (The curves of D_c vs $\log(E_0)$ and D_c vs $1/\phi$ show that the behavior of highly concentrated ceramic suspensions follows the expected relationships in Eq. (2), provided that Q does not depend on ϕ.)

For scattering in highly turbid suspensions, the influence of the extinction coefficient efficiency, volume fraction solids, and exposure dose on the cure depth will be determined for the ceramic suspensions in this work, therefore aiding in the prediction of cure depth for any UV-curable ceramic suspension.

IV. THE EXTINCTION COEFFICIENT EFFICIENCY Q

The dimensionless function Q embodies a complex physics for scattering behavior in a dense system. In general, one might expect Q to depend on ϕ, $\langle d \rangle$, and the ratio $m = n_p/n_0$, with[2]

$$Q(\phi, x, m) = (m-1)^2 \tilde{Q}(\phi, x, m) = (\Delta n/n_0)^2 \tilde{Q}(\phi, x, m), \tag{3}$$

where $x = \pi\langle d \rangle/\lambda$, n_p is the particle refractive index, n_0 is the UV-curable solution refractive index, and Δn is the difference between the two.

There are several closed-form equations for Q[23–25] in terms of x and ρ, where ρ is related to the refractive index difference between the ceramic and the UV-curable solution

$$\rho = x\Delta n = x(n_p - n_0).$$

For the present case, the particle size is equal to or greater than the wavelength of radiation, so Rayleigh scattering is not appropriate for Q.[23]

TABLE III. Refractive index dependence on the scattering efficiency term Q for turbid silica suspensions; a comparison between the experimental value and three theoretical values. Values used in Eq. (2) for Q_{exp}: $\langle d \rangle = 2.29$ μm, $n_p = 1.56$ (at $\lambda = 366$ nm), $E_0 = 1500$ mJ/cm^2, $E_{crit} = 20$ mJ/cm^2, $\phi = 0.50$.

UV-curable solution	n_0	D_c (μm)	Q_{exp}	Q_{ray}	Q_{mie}	Q_n
Aq #1	1.38	250	0.053	6.09	2.12	0.017
Aq #2	1.40	340	0.039	5.00	1.82	0.013
Aq #3	1.41	450	0.030	4.06	2.16	0.011
Aq #4	1.42	490	0.027	3.64	2.00	0.010
Aq #5	1.44	700	0.019	2.42	2.20	0.007
diacrylate	1.46	760	0.017	2.03	2.03	0.005

In the Rayleigh–Gans region, Q_{ray} is a strong function of x and the square of the refractive index difference, Δn^2, as shown in the equation below:

$$Q_{ray} = \tfrac{1}{2}\rho^2 = \tfrac{1}{2}x^2\Delta n^2.$$

However, for Q_{ray} to be valid, the term ρ must be $\ll 1$, corresponding to a small difference in the refractive indices: scattering occurs but not to a significant degree. Therefore, Q must be much less than 1.

The particle size and refractive index difference can be very large for the case of Mie scattering, where

$$Q_{mie} = 2 - \frac{4\sin\rho}{\rho} + \frac{4}{\rho^2}(1 - \cos\rho).$$

Nevertheless, the overall magnitude of Q_{mie} is small. The Mie Q is an oscillating function of ρ, where for large x, Q_{mie} approaches a value of 2.

Theoretical forms for Q will be compared to experimental results using Eq. (2). By determining the scattering behavior through the term Q, the cure depth behavior for turbid ceramic suspensions will be understood. Only the silica and alumina suspensions will be discussed in detail. Results and discussions for these suspensions can be applied to the silicon nitride suspension.

A. The function Q for silica suspensions

1. Dependence on refractive index of the UV-curable solution

The extinction coefficient efficiency Q embodies the scattering behavior for turbid suspensions. In Table III, experimental values for Q are compared with calculated forms for all silica-UV solutions. An additional form for Q, similar to Eq. (3), will be considered, in which the predominant behavior is a scaling with the square of the refractive index difference, or $Q_n = \Delta n^2/n_0^2$. The average particle size is used even though the silica powder has a wide particle size distribution; a more rigorous treatment of particle size effects will not change the overall trends in the cure depth behavior.[23] The value for E_{crit} was set to 20 mJ/cm^2 for all UV-curable solutions.[26–28]

Looking at Fig. 2(a), a linear fit is expected as Δn^2 decreases (e.g., $D_c \uparrow$ as $\Delta n^2 \downarrow$). Forms of Q, which expect a large influence on the square of the refractive index difference, Q_{ray} and Q_n, show the expected linear behavior where

TABLE IV. Dose dependence on the scattering efficiency term Q for a turbid silica suspension: a comparison between the experimental value and three theoretical values. Values used in Eq. (2) for Q_{exp}: $\langle d\rangle = 2.29$ μm, $n_p = 1.56$ (at λ=366 nm), $E_{crit} = 20$ mJ/cm², $\phi = 0.50$, $n_0 = 1.42$ (at λ=366 nm).

E_0 (mJ/cm²)	D_c (μm)	Q_{exp}	Q_{ray}	Q_{mie}	Q_n
380	400	0.023			
600	425	0.024			
860	460	0.025			
1500	490	0.027	3.64	2.00	0.010
2200	540	0.027			
5100	630	0.027			

D_c is proportional to $1/Q$ or $1/\Delta n^2$. However, the square of the refractive index difference form of Q, Q_n, best matches the experimental results as shown in Table III. General observations show the Rayleigh–Gans equation for Q is not strictly valid since the values are greater than one. Mie theory will not produce a linear fit if the cure depth is plotted against $1/Q_{mie}$. So the square of the refractive index difference is the major factor influencing the depth of cure for turbid suspensions and the particle size term x^2 must be a minor influence given that the Rayleigh–Gans form for Q does not explain the scattering behavior.

2. Dependence on dose

From Fig. 2(a), the experimental extinction coefficient, Q_{exp}, can be determined and compared with the three theoretical forms: Q_{ray}, Q_{mie}, and Q_n. Table IV shows the results for the aqueous UV-curable solution with a refractive index of 1.42. Once again, the square of the refractive index difference form of Q best matches the experimental results, where Q_{exp} ranges from 0.023 to 0.027, and $Q_n = 0.010$.

The silica suspensions are best described by the square of the refractive index difference form of the scattering efficiency, Q_n, where $Q_n = \Delta n^2/n_0^2$.

B. The term Q for alumina suspensions

1. Dependence on refractive index of the UV-curable solution

From Table V, the magnitude of the scattering efficiency term, Q_n ($Q = \Delta n^2/n_0^2$), best matches the experimental results for a variety of UV-curable solutions. Even though the square of the refractive index difference, Δn^2, best describes the scattering behavior, it does not determine the effect of particle size. With Eq. (2) and assuming $Q = \Delta n^2/n_0^2$, it is expected that the cure depth is proportional to the particle size, where $D_c \propto \langle d\rangle$. However, the results in Fig. 1(b) show the opposite effect. The term Q must include particle size effects on cure depth behavior in turbid suspensions.

TABLE VI. Dose dependence on the scattering efficiency term Q for a turbid alumina suspension: a comparison between the experimental value and three theoretical values. Values used for Q_{exp}: $\langle d\rangle = 0.34$ μm, $n_p = 1.71$ (at λ=366 nm), $E_{crit} = 20$ mJ/cm², $\phi = 0.50$, $n_0 = 1.42$ (at λ=366 nm).

E_0 (mJ/cm²)	D_c (μm)	Q_{exp}	Q_{ray}	Q_{mie}	Q_n
390	381	0.0035			
660	402	0.0039			
1100	417	0.0044	0.34	2.19	0.042
1800	430	0.0047			
2900	452	0.0050			

2. Dependence on dose

From Fig. 2(b), the experimental coefficient efficiency term can be determined and compared with the three theoretical forms as shown in Table VI. Once again, the square of the refractive index difference form, $Q_n = \Delta n^2/n_0^2$, best matches the experimental results.

The alumina results show that Q_n best describes the scattering behavior for turbid suspensions but does not accurately describe the particle size effect.

V. THE $\tilde{Q}$ TERM

With an understanding that the scattering efficiency Q_n best describes the magnitude of the cure depth D_c, it is necessary to discover other factors which influence the cure depth behavior through the term $\tilde{Q}$ in Eq. (3), where

$$Q_{exp} = \frac{2d}{3\phi D_c}\ln\left(\frac{E_0}{E_{crit}}\right) = Q = \tilde{Q}\frac{\Delta n^2}{n_0^2},$$

or

$$\tilde{Q} = \frac{n_0^2}{\Delta n^2}\frac{2d}{3\phi D_c}\ln\left(\frac{E_0}{E_{crit}}\right). \tag{4}$$

The term $\tilde{Q}$ may be a function of the volume fraction (ϕ), the particle size (x), the dose (E_0), and the square of the refractive index difference (Δn^2); its behavior as a function of these variables will be determined.

TABLE V. Refractive index and particle size dependence on the scattering efficiency term Q for turbid alumina suspensions: a comparison between the experimental value and three theoretical values. Values used for Q_{exp}: $n_p = 1.71$ (at λ=366 nm), $E_0 = 1500$ mJ/cm², $E_{crit} = 20$ mJ/cm².

Alumina	UV-curable solution	n_0	$\langle d\rangle$ (μm)	ϕ	D_c (μm)	Q_{exp}	Q_{ray}	Q_{mie}	Q_n
AKP-50	Aq #1	1.38	0.46	0.5	400	0.007	0.78	2.2	0.057
AKP-15	Aq #1	1.38	0.61	0.5	300	0.012	1.36	2.93	0.057
RC-HP	Aq #4	1.42	0.34	0.5	450	0.004	0.34	2.19	0.042
RC-HP	Diacrylate	1.46	0.34	0.4	275	0.009	0.25	0.9	0.029
AKP-15	Diacrylate	1.46	0.61	0.5	370	0.010	0.81	2.24	0.029

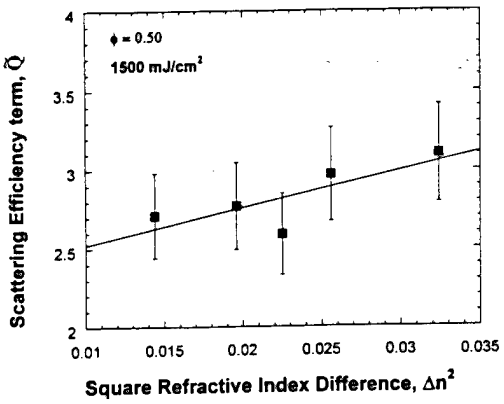

FIG. 3. The experimental scattering efficiency term $\bar{Q}$ as a function of the refractive index difference (Δn^2) for 0.50 solids loading silica in the five aqueous solutions.

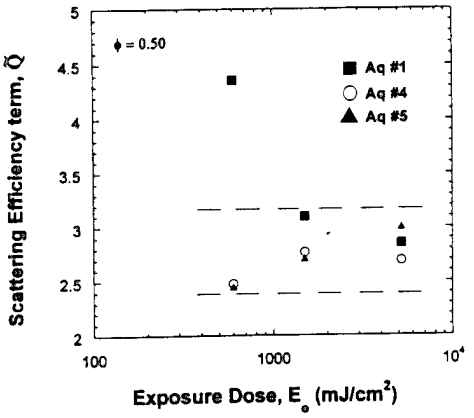

FIG. 5. The experimental scattering efficiency term $\bar{Q}$ as a function of the exposure dose (E_0) for 0.50 solids loading silica in three aqueous solutions.

A. Experimental values for silica suspensions

1. Refractive index difference dependence

Figure 3 shows the influence of refractive index difference on the term $\bar{Q}$. Looking at the data for high solids aqueous silica suspensions, the value for $\bar{Q}$ varies between 2.5 and 3.0. The value rises slightly as the refractive index difference increases, or where more scattering behavior is expected.

2. Volume fraction dependence

Fig. 4 results in two general behaviors (the influence of volume fraction on the term $\bar{Q}$). Both curves show linear behavior, but the addition of solids in the UV-curable suspension with a refractive index of 1.44 (Aq#5) strongly affects the value for $\bar{Q}$. Since the square of the refractive index difference, Δn^2, decreases by 50% in comparison to Aq#1, there must be a transition from absorption to scattering dominated behavior as the solids content increases. This will be discussed in a later section. Note, at high solids contents, the value for $\bar{Q}$ varies between 2 and 3, similar to the results for the refractive index difference dependence.

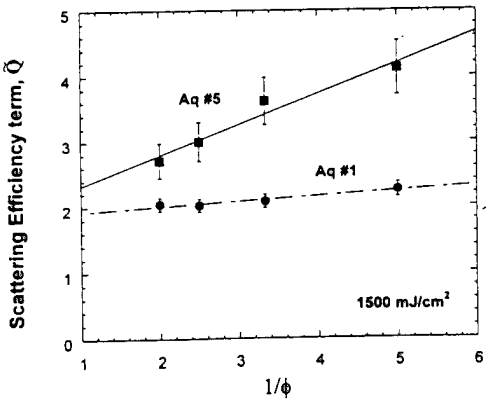

FIG. 4. The experimental or expected scattering efficiency term $\bar{Q}$ as a function of volume fraction ($1/\phi$) for silica dispersed in two aqueous UV-curable solutions (Aq #1 and Aq #5).

3. Dose dependence

In Fig. 5, the dose dependence on the term $\bar{Q}$ has similar results, where the value varies between 2.5 and 3.25. At one low dose, there is an inconsistent data point for silica in the UV-curable aqueous suspension with a refractive index of 1.38 (Aq#1). Possibly the cure depth was measured incorrectly or the polymerization behavior is quite different at low doses in this highly scattering suspension; the rest of the data for three high solids loading aqueous suspensions show similar results.

By looking at three conditions for silica suspensions, the value for $\bar{Q}$ lies between 2 and 3.

B. Experimental values for alumina suspensions

1. Refractive index difference dependence

The effect of the refractive index on the term $\bar{Q}$ will be discussed in relation to the particle size of alumina dispersed in the UV-curable suspensions. Table VII shows the experimental values for $\bar{Q}$ in relation to the refractive index difference for three 0.50 solids loading suspensions. The value of $\bar{Q}$ ranges between 0.131 and 0.238. As expected, the value for $\bar{Q}$ decreases when smaller particle size alumina is used in the same suspension ($D_c \propto 1/\bar{Q}$).

2. Volume fraction dependence

Figure 6 shows the dependence of volume fraction on $\bar{Q}$, where at high solids loading, the value varies between 0.12 and 0.35 for the three solutions discussed in the previous

TABLE VII. Experimental values for $\bar{Q}$ as a function of the refractive index difference and particle size. Values used for $\bar{Q}$: n_p=1.71 (at λ=366 nm), E_0=1500 mJ/cm², ϕ=0.50.

Alumina	UV-curable solution	n_0	$\langle d \rangle$ (μm)	D_c (μm)	$\bar{Q}_{exp}$
AKP-50	Aq #1	1.38	0.46	400	0.134
AKP-15	Aq #1	1.38	0.61	300	0.238
RC-HP	Aq #4	1.42	0.34	420	0.131

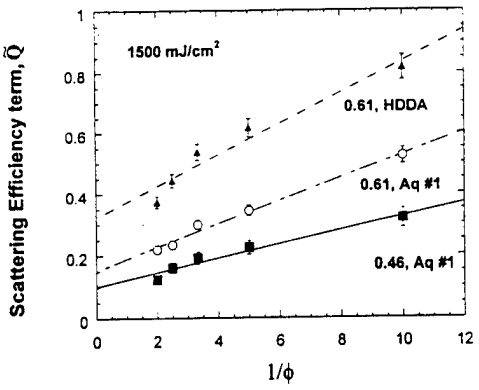

FIG. 6. The experimental scattering efficiency term $\tilde{Q}$ as a function of volume fraction ($1/\phi$) for alumina dispersed in three UV-curable solutions.

section. All solutions have a strong dependence on volume fraction, where the scattering increases as more particles are added to the suspension.

3. Dose dependence

For alumina powder with an average particle size of 0.34 μm dispersed at a solid loading of 0.50 in the aqueous suspension with a refractive index of 1.42 (Aq#4), there is an increasing value for $\tilde{Q}$ as the exposure dose increases as shown in Fig. 7. The value of $\tilde{Q}$ varies between 0.080 and 0.140 as the exposure dose increases from 400 to 4000 mJ/cm^2.

The alumina suspensions show a wider range of values for $\tilde{Q}$, which is expected for the variance in the particle sizes, where $0.10<\tilde{Q}<0.35$.

C. $\tilde{Q}$ as a function of particle size

Without taking the particle size into account, Q (from Q_n) predicted the scattering behavior of the silica solutions, but did not accurately describe the alumina data. The results for alumina show as the particle size became finer, the cure depth increased. In contrast, Eq. (2), when $Q=\Delta n^2/n_0^2$ is substituted, predicts the cure depth should increase with increasing particle size.

For the extinction coefficient efficiency equation, $Q=\tilde{Q}\Delta n^2/n_0^2$, the term $\tilde{Q}$ is expected to contain the particle

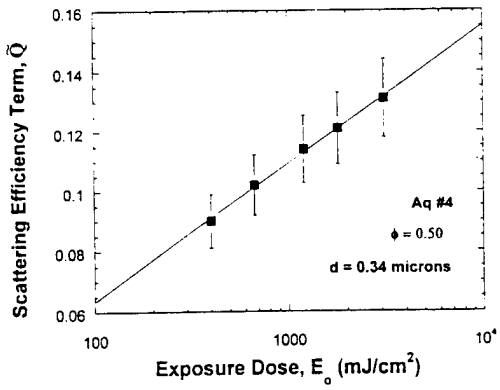

FIG. 7. The experimental scattering efficiency term $\tilde{Q}$ as a function of the exposure dose (E_0) for 0.50 solids loading alumina in aqueous solution #4.

TABLE VIII. Comparison of the experimental value for $\tilde{Q}$ to the calculated value.

Ceramic	Experimental value $\tilde{Q}_{exp}$	$\langle d \rangle$ (μm)	Interparticle spacing, S (nm)	Calculated value $\tilde{Q}=S/\lambda_0$
silica	$2<\tilde{Q}<3$	2.29	949	2.59
alumina	$0.10<\tilde{Q}<0.35$	0.61	253	0.69
		0.46	191	0.52
		0.34	144	0.39
silicon nitride	0.68	0.44	182	0.49

size-wavelength relationship and its effect on the depth of cure.[2,5] However, the behavior of turbid suspensions could not be described when the particle size was related directly to the wavelength through the term x in the Rayleigh–Gans and Mie formulas for Q. Assuming that the scattering coefficiency term Q is related to d/λ is similar to scattering theories that consider one particle in a medium.[2,5] Experimental results of turbid suspensions show that scattering is dominated by the refractive index difference, not by the particle size. Moreover, at the volume fractions considered in turbid suspensions, the relationship to be considered is the interparticle spacing, not the particle size. The spacing between particles will affect how the radiation penetrates the suspension, where interference effects as well as absorption by the photoinitiator(s) determine the cure distance. This interference phenomenon is complicated[29,30] and cannot be described with simple formulas. With radiation traveling from a variety of directions through an array of finely spaced particles, the resulting interference pattern is difficult to describe and beyond the scope of basic theory.

Using simple cubic packing, the median particle size for ceramics in this study, and a 0.50 solids loading, the interparticle spacing, S, is calculated in Table VIII. For the silica suspensions with a large particle size, the interparticle spacing is 950 nm, which is several times larger than the UV wavelength. For the alumina suspensions using fine particles, the spacing varies from 140 to 250 nm which is less than the UV wavelength. With $\tilde{Q}\propto S/\lambda$ and $\lambda=366$ nm, $\tilde{Q}>1$ for the silica suspensions (coarse powder), and $\tilde{Q}<1$ for the alumina suspensions (fine powders).

Also shown in Table VIII, are the experimental values for $\tilde{Q}$ from the data using Q. The value of $\tilde{Q}$ is difficult to understand in terms of d/λ, but in terms of S/λ, turbid suspensions can be described by Eq. (2). For example, the silica suspensions are described by Eq. (2), when the value of $\tilde{Q}$ is between 2 and 3. With $\tilde{Q}=S/\lambda$, the value of $\tilde{Q}=2.59$.

In the case of alumina, the value of $\tilde{Q}$ must be roughly between 0.10 and 0.35 for 0.50 solids loading suspensions, and with $\tilde{Q}=S/\lambda$, the calculated range is $0.39<\tilde{Q}<0.69$. This reasonably describes the alumina suspensions, where the interparticle spacing dominates over particle size in predicting the depth of cure. Moreover, the difference in cure depth related to particle size can be explained using the particle spacing, S, where smaller particle size results in a smaller $\tilde{Q}$ value, and therefore the cure depth increases.

Even though the silicon nitride data has not been discussed, Table VIII shows that $\tilde{Q}=S/\lambda$ reasonably describes the scattering behavior for this highly turbid suspension. Note, the square of the refractive index difference, Δn^2, is still the major determinant for the magnitude of the depth of cure.

VI. DISCUSSION

A. Quantitative prediction of D_c

With $Q=\Delta n^2/\Delta n_0^2$, *the magnitude of the cure depth can be predicted for high solids loading turbid suspensions. However, by looking at the curves in Figs. 5 and 7, there is a noticeable effect that the dose has on the value* $\tilde{Q}$. Moreover, the volume fraction dependence shows different behaviors in Figs. 4 and 6. The theoretical equation for turbid suspensions describes the cure depth behavior well, but an absorption term should be included, where the absorption term would describe behaviors related to the absorption limited region and/or dilute limit in these suspensions and is dependent upon the photochemistry of the UV-curable solution. To determine this behavior, polymerization research at low volume fractions must be investigated.

We propose a general scattering equation that describes the cure behavior for nonabsorbing ceramic powders dispersed in ultraviolet curable solutions:

$$D_c=\frac{2\langle d\rangle}{3\tilde{Q}}\frac{n_0^2}{\Delta n^2}\ln\left(\frac{E_0}{E_{\text{crit}}}\right),$$

where

$$\tilde{Q}\propto\frac{S}{\lambda}. \tag{5}$$

This model of scattering behavior is a simple model for understanding the magnitude of the cure depth for turbid suspensions where absorption does not play a major role. Refinement of the model is best handled, first by the addition of an absorption term. Further physical understanding of the cure depth behavior should consider more complex theories. For example, diffuse wave spectroscopy[30] is not constrained to low volume fractions for the description of radiation traveling through a suspension. This theory can describe the scattering behavior of concentrated suspensions, but needs to include an absorption term for the polymerization of the medium. Further research will refine the basic model in this work and incorporate other theories.

B. Predicting cure depth for other ceramics

Figure 8 shows the refractive index versus density for a variety of ceramic materials. Superimposed on the graph are the refractive indices for water, the diacrylate, and methyl naphthalene. Water represents a low refractive index solvent and methyl naphthalene has one of the highest refractive indices for common solvents which are not too chemically hazardous.

Quartz silica is a ceramic material with a low refractive index, thereby achieving large cure depths at high solids loadings when dispersed in aqueous UV-curable solutions. With silicon nitride acceptable cure depths ($D_c=200$ μm stereolithography requirement) were not achievable due to the large refractive index difference between the ceramic and diacrylate. If the theoretical scattering equation is fit to the experimental data at 0.50 volume fraction solids so as to calculate the absolute cure depth (40 μm), one can determine the refractive index needed to obtain a cure depth of 200 μm at large doses. The value for the UV-curable solution would be 1.66, and methyl naphthalene is a good candidate. By tuning the refractive index difference, the cure depth can be modified to the user's choice.

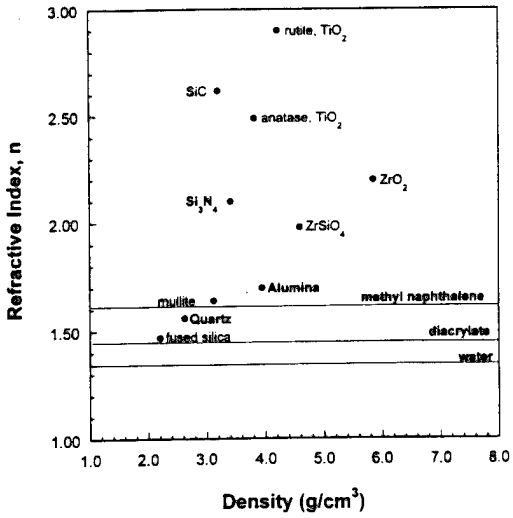

FIG. 8. Refractive index for a variety of ceramic materials in comparison with the refractive indices for two solvents (water and methyl naphthalene) and the diacrylate.

VIII. CONCLUSIONS

The effective Beer's law equation [Eq. (2)] accurately describes the cure depth behavior for highly turbid, ultraviolet-curable suspensions, with linear proportional relationships for cure depth versus $1/\phi$ and cure depth versus $\log(E_0)$. This validates the derivation of the scattering equation using Beer's law as a starting point.

For the extinction coefficient efficiency term Q, $Q=\tilde{Q}(\Delta n^2/n_0^2)$, best represents the data as the factor controlling the depth of cure. Neither the Rayleigh–Gans nor Mie formulas predict the scattering behavior. With $Q=\Delta n^2/n_0^2$ inserted into the scattering equation, the magnitude of expected cure depth for any nonabsorbing ceramic powder dispersed in the aqueous or diacrylate solution can be predicted.

For turbid suspensions, scattering-limited cure depths do not appear to be simply related to particle size. Rather, the interparticle distance, S, appears to influence the resulting cure depth through the term $\tilde{Q}$, where $\tilde{Q}\propto S/\lambda$.

ACKNOWLEDGMENTS

We thank the sponsors, Dr. Steve Fishman and Dr. Ralph Wachter, at the Office of Naval Research for funding this work under contract N00014-913-1-0302. We are grate-

ful to Dr. Paul Jacobs, Dr. Thomas Pang, and Kelly Kwo, at 3D Systems, in Valencia, CA, for their time and use of their stereolithography apparatus. The authors also wish to express their gratitude to the referee for the thorough reviews and helpful comments.

[1] C. E. Bohren and D. R. Huffman, *Absorption and Scattering of Light by Small Particles* (Wiley, New York, 1988).
[2] H. C. van de Hulst, *Light Scattering by Small Particles* (Wiley, New York, 1957).
[3] H. Jacobowitz, J. Quant. Spectrosc. Radiat. Transf. **11**, 691 (1971).
[4] H. C. van de Hulst, *Multiple Light Scattering: Tables, Formulas, and Applications*, (Academic, New York, 1980), Vol. 2, Chap. 10.
[5] P. W. Barber and S. C. Hill, *Light Scattering by Particles: Computational Methods* (World Scientific, Teaneck, NJ, 1990).
[6] H. Blumer, Z. Phys. **32**, 119 (1925).
[7] M. Kerker, *The Scattering of Light and other Electromagnetic Radiation* (Academic, New York, 1969).
[8] M. L. Griffith and J. W. Halloran, *Manufacturing Science and Engineering*, (American Society of Mechanical Engineers, New York, 1994), Vol. 68-2, pp. 529–534.
[9] M. L. Griffith and J. W. Halloran, *Proceedings of the Solid Freeform Fabrication Symposium*, Austin, TX, August 8–10, 1994, edited by H. Marcus *et al.* (University of Texas, Austin, 1994), pp. 396–403.
[10] M. L. Griffith and J. W. Halloran, *Proceedings of the Sixth International Conference on Rapid Prototyping*, Dayton, OH, June 4–7, 1995, edited by A. Lightman *et al.* (University of Dayton, Dayton, OH, 1995).
[11] M. L. Griffith, T-M Chu, W. Wagner, and J. W. Halloran, *Proceedings of the Solid Freeform Fabrication Symposium*, Austin, TX, August 7–9, 1995, edited by H. Marcus *et al.* (University of Texas, Austin, TX, 1995), pp. 31–38.
[12] C. Hull, U.S. Patent No. 4,575,330 (1986).
[13] P. F. Jacobs, *Rapid Prototyping and Manufacturing: Fundamentals of Stereolithography*, (Society of Manufacturing Engineers, Dearborn, MI, 1992).
[14] T. H. Pang, *Proceedings of the Solid Freeform Fabrication Symposium*, Austin, TX, August 8–10, 1994, edited by H. Marcus *et al.* (University of Texas, Austin, TX, 1994), pp. 204–224.
[15] M. L. Griffith and J. W. Halloran, J. Am. Ceram. Soc. **79**, 2601 (1996).
[16] Michelle Lynn Griffith, Ph.D. thesis, University of Michigan, Materials Science and Engineering Department, March, 1995, Chap. 4 and 5.
[17] E. D. Pawlik, *Handbook of Optical Constants of Solids*, (Harcourt Brace Jovanovich, New York, 1985), pp. 749–764, 771–774.
[18] C. L. Haertling, S. Yoshikawa, and R. R. Newnham, J. Am. Ceram. Soc. **73**, 3330 (1990).
[19] A. C. Young, O. O. Omatete, M. A. Janney, and P. A. Menchofer, J. Am. Ceram. Soc. **74**, 612 (1991).
[20] O. O. Omatete, M. A. Janney, and R. A. Strehlow, Am. Ceram. Soc. Bull. **70**, 1641 (1991).
[21] S. P. Pappas, *Radiation Curing: Science and Technology*, edited by S. P. Pappas, (Plenum, New York, NY, 1992), pp. 1–20.
[22] H. C. van de Hulst, *Light Scattering by Small Particles*, Sec. 2.6 (J. Wiley, New York, NY, 1957).
[23] H. C. van de Hulst, *Light Scattering by Small Particles*, (J. Wiley, New York, NY, 1957), Chap. 10 & 11.
[24] T. Allen, *Particle Size Measurement*, (Chapman and Hall, New York, 1990), pp. 491–494.
[25] R. J. Hunter, *Introduction to Modern Colloid Science* (Oxford Science, Oxford, 1993), pp. 80–87.
[26] C. E. Habermann, *Encyclopedia of Chemical Technology*, 4th ed. (1991), pp. 251–266.
[27] Chemistry of Acrylamide, Bull. PRC 109, Process Chemicals Department, American Cyanamid Co., Wayne NJ, 1969.
[28] C. E. Hoyle, *Radiation Curing: Science and Technology* (Plenum, New York, NY, 1992), pp. 273–299.
[29] Basic physics describes plane waves traveling through two widely separated slits that act as point sources for setting up constructive and destructive interference patterns.
[30] D. A. Weitz and D. J. Pine, *Dynamic Light Scattering: The Method and some Applications*, edited by W. Brown (Oxford University, Oxford, 1993), Chap. 16, pp. 652–720.

CERAMIC STEREOLITHOGRAPHY FOR INVESTMENT CASTING AND BIOMEDICAL APPLICATIONS

Michelle L. Griffith, Tien-Min Chu, Warren Wagner and John W. Halloran
Materials Science and Engineering Department, College of Engineering
and Biologic and Materials Sciences Department, School of Dentistry
The University of Michigan
Ann Arbor, MI

ABSTRACT

Ceramic green bodies can be created using stereolithography methods by using an ultraviolet curable suspension of ceramic powders in place of the usual resin -a "ceramic resin". We are developing ceramic resins from hydryoxyapatite ceramics, to enable custom made ceramic implants by SLA, and from silica and alumina, to enable metal casting molds by SLA. We demonstrate SLA of silica, a model refractory for metal casting molds, and SLA of alumina, which present the rheological behavior and UV curing properties of several "ceramic resins", and discuss silica parts made on an SLA-250.

INTRODUCTION

Conventional StereoLithography [SLA] is used to build plastic parts from ultraviolet (UV) -curable organic resins. In the past two years, we have developed techniques to apply SLA to directly make ceramics[1,2]. Ceramic powder is dispersed in a fluid UV-curable monomer to prepare a ceramic/UV-curable monomer suspension, which we call a "ceramic resin". The building process is the same as conventional SLA. As the UV laser scans the "ceramic resin", the monomer solution is cured forming a ceramic-polymer composite layer. Layer by layer, the three-dimensional model is made from this ceramic-polymer composite to create a shaped "green" ceramic. After the building, the green ceramic object is heated in a furnace to remove polymer and sinter the final ceramic.

This paper presents progress on two ceramic SLA projects. One project [involving TMC] is concerned with the fabrication of custom-made hydroxyapatite (HA) ceramic implants. The other project [by MLG] involves fabrication of refractory ceramics. For both, the key issue is the preparation of an appropriate ceramic resin that has a viscosity low enough to use in an SLA [about 3,000 cps or less] and a curing depth sufficient for typical layer thickness [at least 200 μm].

Our long range goal for custom-made ceramic implants will build implants from CT scans, using methods developed for surgical models [3], with the implant is designed and built from hydroxyapatite by SLA. Hydroxyapatite has been used in the clinics in the bulk form for bone substitutes or as coatings for metallic implants for about 20 years[4] for its ability to form a direct contact with the regenerated bone tissue[5-7].The first step, reported here, is the development of an HA ceramic resin has the appropiate rheology and cure behavior, and which can be patterned and fired without degrading the hydroxyapatite. For refractory ceramics, our long range goal is to directly fabricate ceramic investment casting shells and cores by SLA. We report on the SLA properties of a silica resin and an alumina resin.

Ceramic resins have the same relationship between cure depth, C_d, and the energy dose, E, as conventional resins, although the mechanism of attenuation is different. Instead of adsorption, cure depth is limited by scattering of the UV radiation, since ceramic suspensions are turbid. The cure depth for ceramic suspensions can be related to the properties of the resin by:

[1] $$C_d \propto \frac{\beta}{\phi} \frac{d}{\Delta n^2} \ln\left[\frac{E}{E_c}\right]$$

The penetration depth is controlled by the particle size (d), is inversely proportional to the volume fraction (ϕ) of ceramic and strongly dependent upon refractive index difference between the ceramic and the UV-curable solution, Δn. The critical energy dose, E_C, is the minimum does required to gel the suspension. The term β involves the interparticle spacing and the UV wavelength, but is not yet well understood.

MATERIALS SYSTEMS

Ceramic Resins

The ceramic resins were made by dispersing ceramic powders in a water-based UV-curable solution consisted of acrylamide and methylene bisacrylamide monomers (2), which are similar to gel casting formulations used for molding ceramics(8). The refractive index was adjusted in the range of 1.382-1.441. The silica resin was made from powder with a broad size distribution large average particle size of 2.3 microns. The refractive index of silica is 1.56. The alumina powder was commercial sinterable powder with a average particle size of 0.34 microns. The refractive index of alumina is 1.76. The commercial hydroxyapatite powder had a submicron primary particle size, but was agglomerated into porous 10-40 micron secondary particles.
the alumina and silica were dispersed in the solution at a solids loading of 50 volume percent, producing suspensions with viscosity less than 500 mPa-s [at 3 sec^{-1}], using polyelectolyte dispesants. The HA was more difficult to disperse. Consequently its viscosity was measured as a function of pH and concentration of an anionic polyacryalate dispersant. A mixture of photointiators were used in the formulation: 0.4 w/o phosphine oxide and 0.7 w/o ketone derivative, which is the maximum solubility of these photoinitiators in water. These were added as the last step prior to use.

EXPERIMENTAL

The viscosity of a suspension with 20 vol% of HA powder in the monomer solution was determined with a Brookfield DV-II+ viscometer at 60 rpm.prepared. The pH value of each sample was adjusted with ammonium hydroxide in the range of from 4 to 8. An anionic surfactant (Phreeguard 1000N%) dispersant was added incrementally and the viscosity was measured Iso-viscosity lines were mapped at different combinations of dispersant dose and pH. With this iso-viscosity plot, the range of the pH value and the dose of the dispersant to produce the lowest viscosity of the suspension was defined.

Initial testing of the cure properties were done with a Hanovia conveyorized desktop UV-curing apparatus with a UV lamp@ The two strongest lines emitted by the lamp, 313 nm and 366 nm, correspond closely to the wavelengths used in SLA machines, 312 nm for the He-Cd laser and 351 nm for the Ar-ion laser. The exposure was determined by using a radiometer. After

---

% Calgan Corp. Pittsburgh, PA

@ Hanovia UV Laboratory System, Hanovia, Newark, NJ

exposure, the polymerized sample was removed from the remaining uncured suspension, and the cure depth was measured by optical or electron microscopy.

Silica and alumina resin were tested in a SLA-250 machine using an Ar-ion laser. The critical exposure (E_c) and penetration depth (D_p), were determined for each suspension with the "windowpanes" test geometry(9) andfit to Equation 1. The Ar-ion laser results agreed the UV lamp data at the same energy density. Several three-dimensional parts were fabricated. The curing properties of the HA suspension were illustrated with the UV lamp apparatus, using a simple mask made in the shape of a cartoon skull.

RESULTS

I. Silica and Alumina

Equation 1 assumes that the cure depth is limited by scattering from the ceramic rather than by adsorption by the photopolymer system. It predicts that cure depth should be inversly proportional to the volume fraction ϕ of the dispersed ceramic. Figure 1 shows that this relation is indeed observed for alumina and silica suspensions in a medium with refractive index of 1.381. If scattering is the limiting factor, Eq. 1 also predicts that the cure depth should vary with $1/\Delta n^2$. This is observed in Figure 2 for a variety of silica uspensions, showing that the refractive index difference is the dominating factor controlling the depth of cure in strongly scattering systems. This is discussed in detail elsewhere (10).

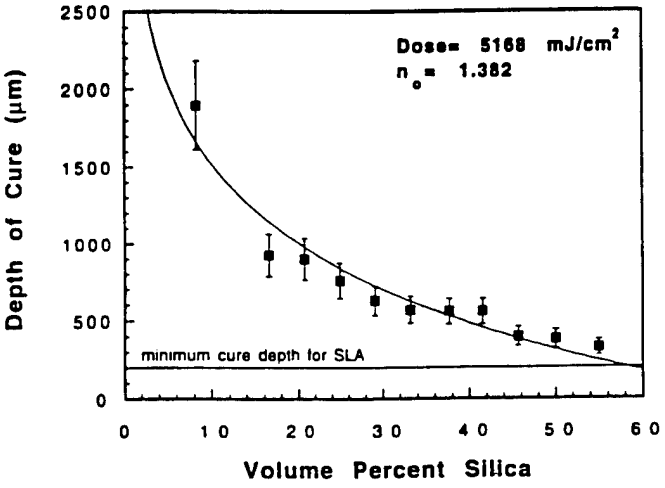

Figure 1 Cure depth vs. inverse volume fraction solids for silica and alumina dispersed in UV-curable solution

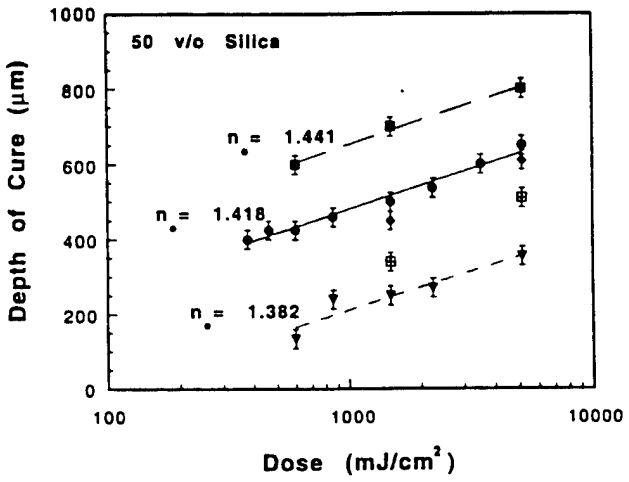

Figure 2 Cure depth vs. refractive index difference for 50 vol% silica in UV-curable solutions

Figure 3 is a photograph of the first three-dimensional ceramic green body fabricated using stereolithography. The object built is a hollow box, 1" x 1" x 0.75", with a 45 degree angle on one side. This was fabricated from 50 v/o silica dispersed in the aqueous solution having a refractive index of 1.418. The SLA parameters used were D_p= 150 µm and E_c= 80 mJ/cm^2. There are 136 layers, each 150 µm thick. The build time for this hollow box was about 4 hours. The sides and the 45 degree angle are built quite accurately. There was no problem with interlayer adhesion. The top of the box is slightly rounded because the recoat blade was not used because the sample was built in an experimental mini-vat. Instead the z-wait time was extended to 45 seconds

to allow the new layer to equilibrate to a reasonably flat surface.The bottom of the box is warped, due to curling of the first layers, probably because of the raster-style build style and inadequate support structure. In spite of the imperfections in this first attempt, we consider this a demonstration of practical ceramic SLA. The silica box was heated to 1000°C to simulate the firing cycle of ceramic molds.

Figure 4 shows the microstructure of an alumina part fabricated on the SLA-250 and subsequently sintered at 1550 °C. This appears to be a high quality dense alumina ceramic, typical of pore-free fine grained alumina ceramics. This demonstrates that SLA-fabricated ceramic green bodies can sinter as readily as conventional ceramics. This is discussed elsewhere (11).

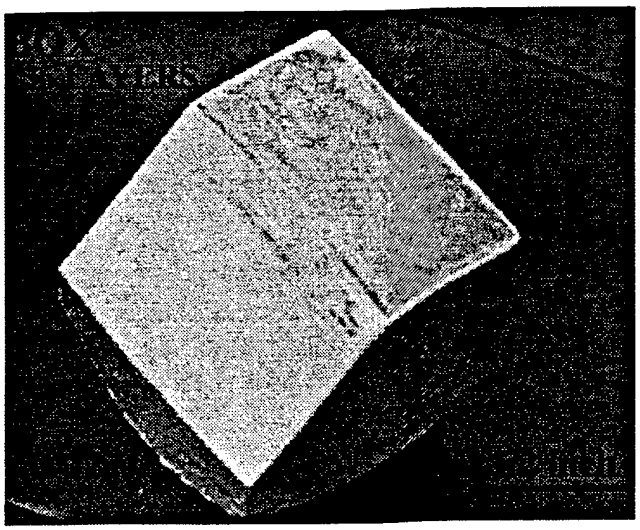

Figure 3 Hollow "box" part fabricated on SLA-250 from silica ceramic resin

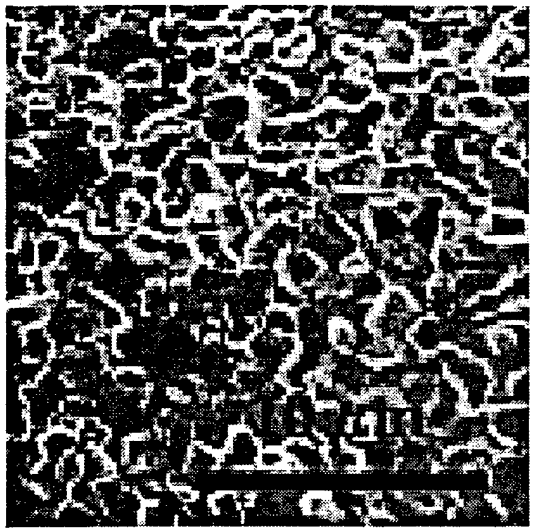

Figure 4 SEM micrograph of the fracture surface of alumina fabricated on SLA-250 sintered 1550°C for 2 hr, showing fine-grained pore-free microstrure

II. Hydroxyapatite

The viscosity of the dispersion of HA powder in acrylamide solution depends upon pH and the amount of polyacrylate dispersiant. A 20 vol% HA-AM/MBAM suspension with 1.46 wt% dispersant equililibrates after mixing to a pH of 6.48. At a constant dispersant dose, viscosity is a minimum around pH 7. Higher dose of dispersant reduces the viscosity over the whole pH range, resulting in a wider low-viscosity region at higher dose of dispersants. Figure 5 shows this behavior as an iso-viscosity plot. After the dose of the dispersant exceeded 2.5 wt% of the dry powder, the viscosity of the suspension in the whole pH range dropped under 100 cps. To establish the effect of HA content, the solids-loading of the suspension was increased from 10 vol% to 45 vol% at a dispersant dose of 3 wt% of dry powder and pH 7, as shown in Figure 6. The viscosity of the suspension increased from 10 cps to 2960 cps. The viscosity of the suspension rose rapidly to above 12,000 cps when the vol% ceramic was increased from 45 vol% to 46.5 vol%.

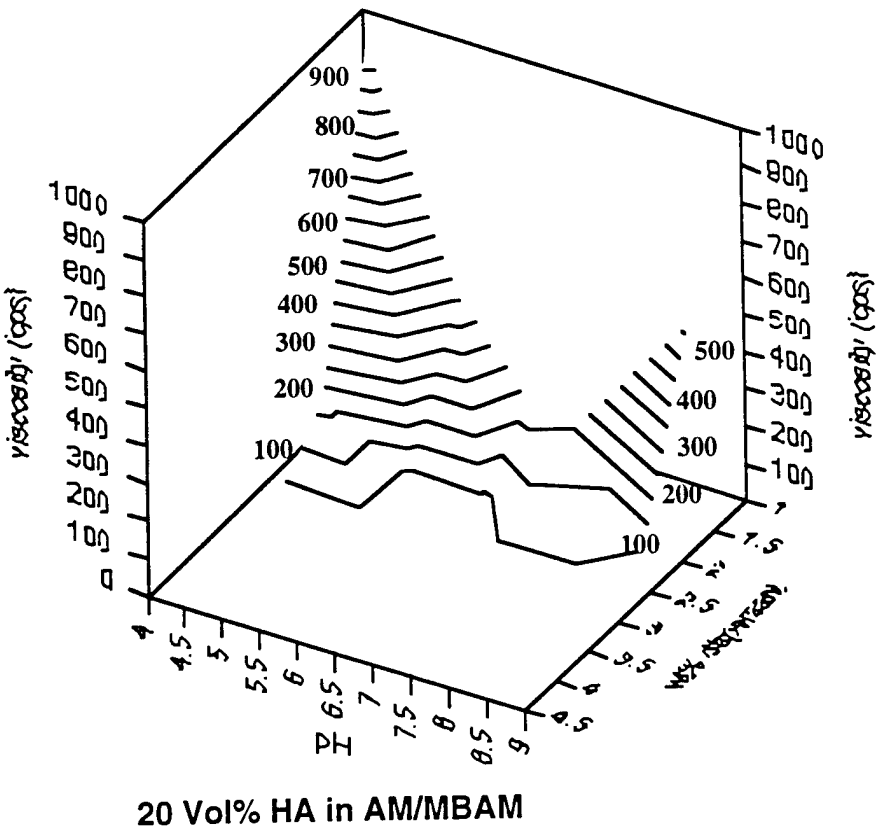

Fig.5 Iso-viscosity contours vs. pH and dispersant dose for 20 vol% HA in AM/MBAM

Cure Depth and Pattern Reproduction

The 45 vol% HA suspension had a cure depth of 280 μm, which is adequate for SLA. The linear relation of cure depth vs. $1/\phi$ is also obeyed for HA powders, as shown in Figure 7. From this we predict that a cure depth larger than 200 μm will be achievable up to 55 vol%. Figure 8 is a demonstration of the pattern reproduction with the HA ceramic resin. On the left is the skull cartoon "mask", made from xeroxed transparency, with the HA /polyacryamide green ceramic layer on the righ. Thechange in the dimension wasdue to the scattering of the light at the edge of the crude xeroxed mask since the light source we used was not a point light source. This should not happen when we use a laser on the SLA-250 machine.

Green Body Property Characterization

The hydroxapatite does not appear to be degraded by this process. Figure 9 is the x-ray diffraction pattern of the hydroxyapatite green body after making the HA ceramic resin, curing, and binder burnout. Only HA is present, which indicates that the hydroxyapatite structure was preserved during the whole process.

CONCLUSIONS

Highly concentrated suspensions of ceramic powders in photopolymerizable solutions can be cured by UV lamps or UV laser. Cure depth is proportional to the logarithm of energy through a Beer-Lambert relation, with the depth of penetration limited by scattering of UV radiation. Depth

of penetration is inversely proportional to ceramic volume fraction and to the square of the refractive index difference between the ceramic and the suspension medium. Multilayer parts have been built using a SLA-250 with an Ar-ion laser, with promising accurate parts with good interlayer adhesion. These first ceramic objects demonstrate the feasibility of stereolithography for directly building green ceramic objects, both for sintered structural ceramic parts and for refractory ceramic shells and cores for metal casting.

The cure depth of a 45 vol% HA suspension was 280 μm, which is above the minimum depth requirement. The hydroxyapatite structure in the green body was retained after polymer binder burnout.

ACKNOWLEDGMENT

This research on refractory ceramics is supported by the Office of Naval Research under grants N00014-93-1-0302 and -95-1-0527, through Dr. S. Fishman and R. Wachter. The biomedical research is supported the the University of Michigan through a Rackham Grant to T-M-Chu. We thank Paul Jacobs, Thomas Pang, and Kelle Kwo of 3D Systems for their help.

REFERENCES

1. M.L. Griffith and J. W. Halloran, *Proceedings of the SFF Symposium,* University of Texas at Austin Publishers, Austin, 1994, pp. 396-403.
2. Michelle L. Griffith, Ph.D. thesis, The University of Michigan, Materials Science and Engineering Department, March 1995.
3. N.G. Stoker, N.J. Mankovich, and D. Valentino, "Stereolithographic Models for Surgical Planning: Preliminary Report," *Journal of Oral and Maxillofacial Surgery*, **50**, 466-471, (1992).
4. L.L. Hench,, "Medical and Scientific Products," In *Engineered Materials Handbook,* Vol. 4, (eds.) J. Samuel J Schneider, The Materials Information Society, 1991, pp. 1007-1013.
5. G. de Lange "The Bone-Hydroxyapatite Interface," In *Handbook of Bioactive Ceramics,* Vol. II, (eds.) T. Yamamuro, L. L. Hench and J. Wilson, CRC Press, Inc., Boca Raton, FL, 1990, pp. 61-75.
6. M. EL Deeb and R. Holmes, "Tissue Response to Facial Contour Augmentation With Dense and Porous Hydroxyapatite in Rhesus Monkey," *Journal of Oral and Maxillofacial Surgery*, **47**, 1282-1289, (1989).
7. C.A.van Blitterswijk, J.J. Grote, W. Kuijpers, W. T. Daems, and K. de Groot, "Macropore tissue ingrowth: a quantitative and qualitative study on hydroxyapatite ceramic," *Biomaterials*, **7**, 137-143, (1986).
8) A.C. Young, O.O. Omatete, M.A.Janney, and P.A. Menchofer,, 1991, " Gel Casting- A New Ceramic Forming Process", *Journal of the American Ceramic Society*, vol. 74, no. 3, pp. 612-618.
9) P.F. Jacobs, *Rapid Prototyping and Manufacturing: Fundamentals of Stereolithography*, Soc. of Manufacturing Engineers, Dearborn, p. 263-281 (1992)
10) M.L. Griffith and J. W. Halloran, "Photopolymerization of Turbid Suspensions", submitted to*Journal of Applicd Physics*
11) M.L. Griffith and J. W. Halloran, "Free Form Fabrication of Ceramics by Stereolithography", submitted to *Journal of the American Ceramic Soc.*

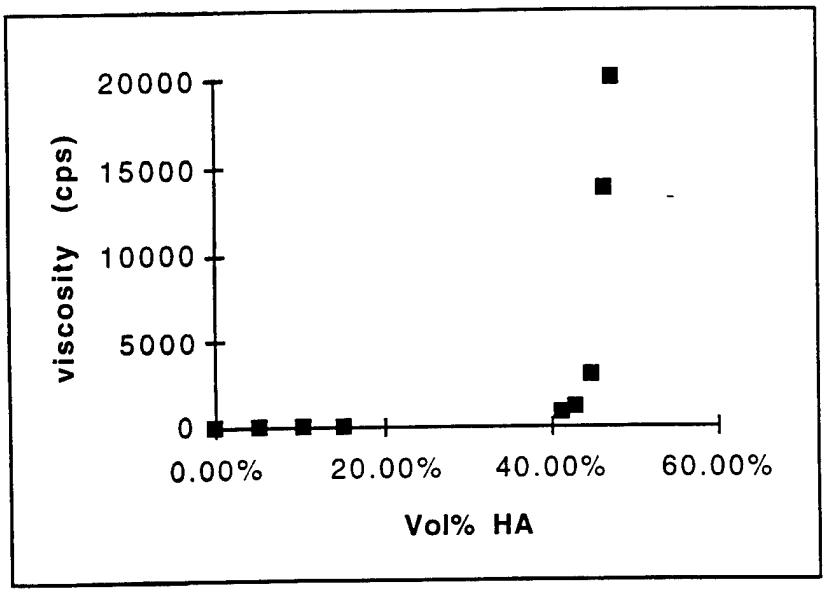

Fig. 2 Viscosity vs. vol% HA with 3 wt% dispersant

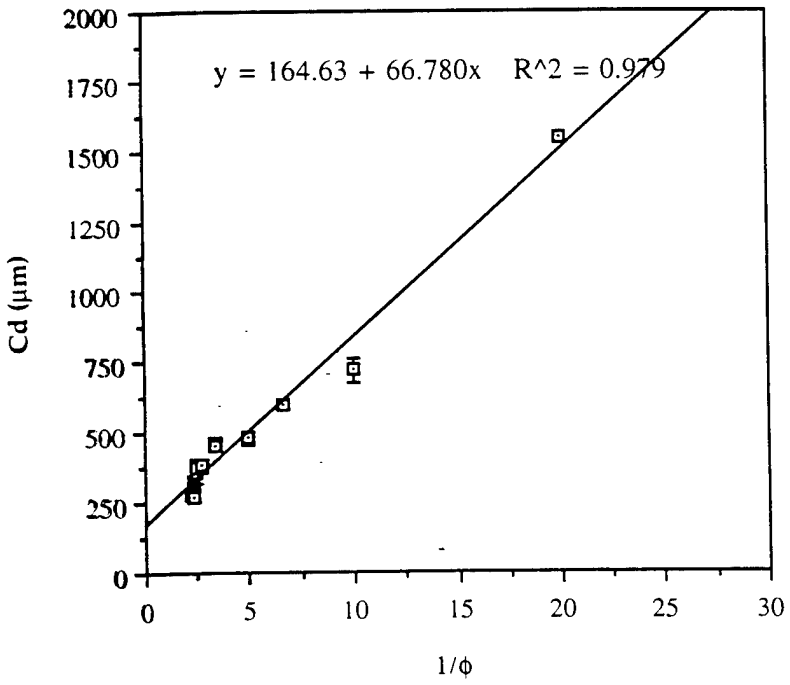

Fig. 7 Cure Depth (µm) vs. 1/ϕ

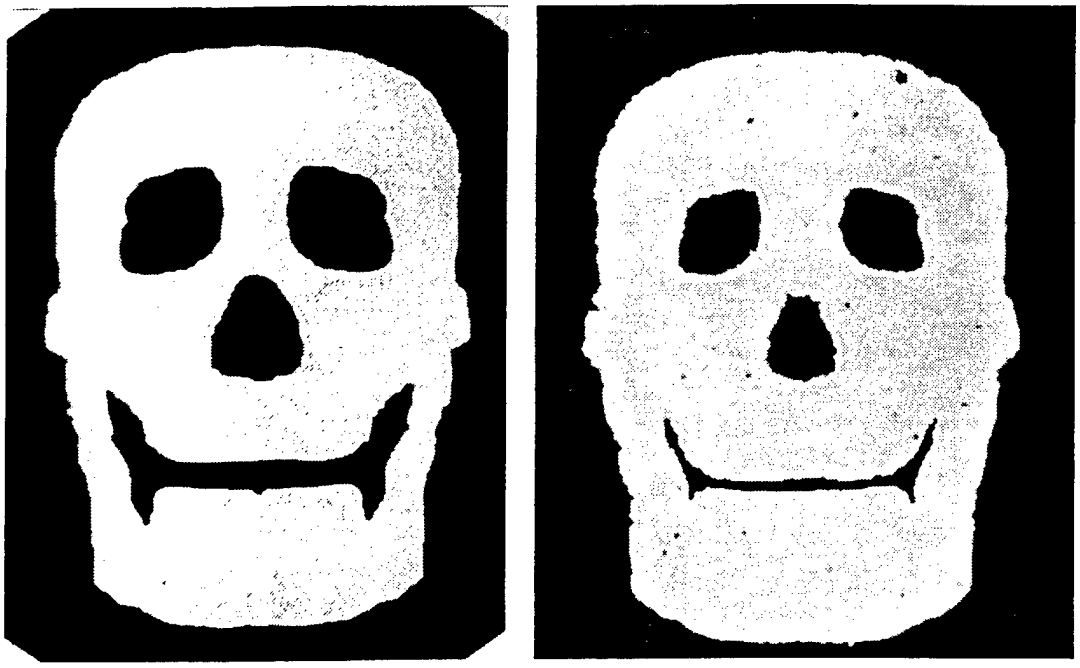

Fig. 8 The test mask (left) and the cured HA/polymer composite layer (right)

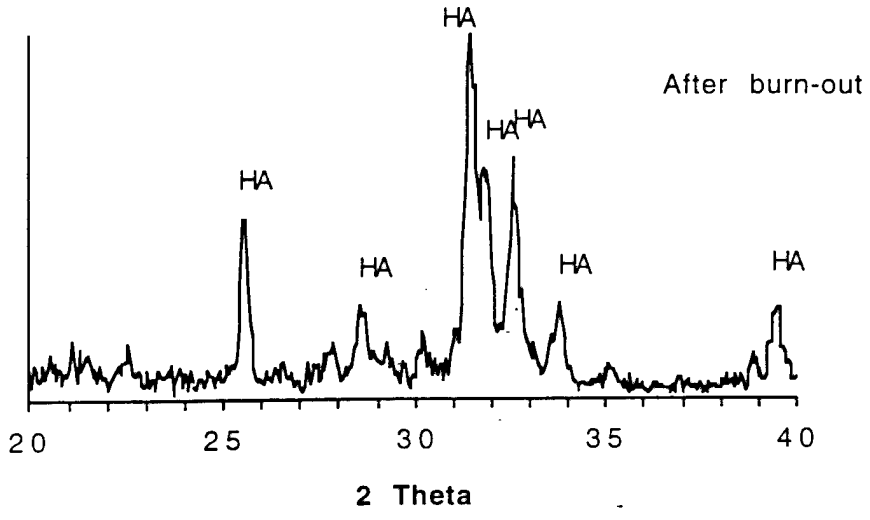

Fig. 9 X-ray diffraction pattern of final hydroxyapatite specimen after polymer binder burn-out

STEREOLITHOGRAPHY OF CERAMICS

Michelle L. Griffith* and John W. Halloran

Department of Materials Science and Engineering, The University of Michigan,
Ann Arbor, MI 48109-2136

Abstract

By dispersing ceramic powders in ultraviolet (UV) curable solutions, stereolithography can fabricate ceramic green bodies. We demonstrate SLA of silica, promising for casting applications using silica, and SLA of alumina which is promising for structural ceramics. Viscosity control for these highly concentrated suspensions and cure depth behavior are the main issues for fabricating a ceramic using stereolithography techniques.

Ceramic SLA suspensions, with low viscosities and large cure depths, were further studied in a stereolithography machine, and three-dimensional parts were built. Part building parameters, D_p and E_c, were determined for this suspension. Layer adhesion and subsequent processing resulted in good ceramic parts.

Introduction

Stereolithography fabricates accurate three-dimensional objects[1]. Unfortunately, the objects can only be produced from polymeric materials. It would be useful to expand the menu of SLA materials. One such area is for the fabrication of ceramics. One can fabricate ceramics by SLA by dispersing ceramic powders within an ultraviolet-curable solution. The UV cured polymer acts as the binder to hold the ceramic particles together before firing. During firing, the polymer is removed and the ceramic powder is sintered, resulting in a ceramic part. This is a promising fabrication method for ceramic shells and cores and for structural ceramic parts.

The two main issues for stereolithography of ceramics are the rheology and the cure depth of concentrated suspensions. A high solids content, about 50 vol%, is required to fabricate a ceramic part. For these highly concentrated suspensions, especially for submicron ceramic powders, the suspension must be colloidally stabilized. This is done by adding the correct dispersants, usually at 1.0 weight percent dry basis. The maximum viscosity for a suspension in the stereolithography apparatus (SLA) is 3000 mPa-s at low shear rates. After a layer is built, the new layer must flow across the old layer, thereby requiring a fluid suspension. Flocculated suspensions, where the particles agglomerate, the viscosity of the suspension increases dramatically at much lower solids loadings. Maintaining low viscosities is difficult as the ceramic powder fraction approaches the Krieger-Dougherty limit[2], usually approaching 0.63 for random packing when the suspension is fluid. The correct dispersants maintain the particles as singlets ensuring the fluidity of the suspension. In this paper, two UV-curable solutions will be discussed, an aqueous and a low viscosity diacrylate. The starting viscosity of the UV-curable solution is important where a lower starting viscosity aids in maintaining a lower viscosity in the concentrated suspension.

The other main issue is the cure depth of the concentrated suspension. With a highly loaded suspension, the ceramic powder will scatter the ultraviolet radiation, thereby

---

* now at Sandia National Laboratory, MS 0958, P.O. Box 5800, Albuquerque, NM 87185

reducing the depth of cure. Below is the scattering equation representing the cure depth behavior for concentrated suspensions:

$$C_d \propto \frac{d}{\phi}\frac{1}{\Delta n^2}\ln\left[\frac{E}{E_c}\right] \qquad \text{Equation 1.}$$

The depth of cure is controlled by the particle size (d), the exposure dose (E), and inversely by the volume fraction (ϕ) and refractive index difference between the ceramic and the UV-curable solution, Δn^2.

With conventional stereolithography resins, the layer thickness is approximately 200 microns, and this was set as the minimum limit for cure depth or layer thickness for the ceramic suspensions. Theoretical aspects relating the cure behavior for a highly concentrated suspension will be discussed later in this paper.

Determining the SLA paramters[3], D_p and E_c, are important for part fabrication. By understanding these two parameters, the layer thickness (C_d) and dose (E) are easily set through the equation derived by Jacobs[3]:

$$C_d = D_p \ln\left[\frac{E}{E_c}\right] \qquad \text{Equation 2.}$$

Preliminary results for freeform fabrication of silica green bodies and the stereolithography parameters will be shown.

Experimental

Table 1 shows the materials used and their properties. Silica has a large average particle size as it is a model material for investment casting. The alumina powder is submicron to ensure correct sintering behavior. A wide variety of aqueous UV-curable solutions were studied to determine the influence of refractive index on the resulting depth of cure. The aqueous solution consisted of acrylamide and methylene bisacrylamide monomers in a aqueous solvent mixture[4,5]. The diacrylate has the highest refractive index, 1.457, and therefore the smallest difference between the ceramic and the UV-curable solution.

In the preparation of a high solids loading ceramic suspension, first the monomers and solvents are mixed for a few minutes in a shear mixer. Then the ceramic powder and dispersants are added incrementally, 5-10 v/o for the ceramic powders and 0.2 w/o dry basis for the dispersant(s), and the suspension is shear mixed between each increment until a solids loading of approximately 30 v/o is achieved. Further addition of ceramic and dispersants is followed by ball milling for complete homogenization and allow the dispersant(s) to stabilize the suspension. After the maximum solids loading is reached, 40-50 vol%, the photoinitiator(s) are added and the suspension is ball milled for roughly five hours. Table 2 shows the ceramic suspensions studied.

After mixing the suspension, the cure properties were investigated using a conveyorized ultraviolet lamp apparatus. Note, the two strongest lines emitted by the lamp, 313 nm and 366 nm, correspond closely to the wavelengths used in SLA machines, 312 nm for the He-Cd laser and 351 nm for the Ar-ion laser. The exposure the sample receives is controlled by the speed of the conveyor belt, and the exposure was determined by using a radiometer for measurement. After exposure, the polymerized sample was removed from the remaining uncured suspension, and the cure depth was measured by optical or electron microscopy.

Promising ceramic suspensions were then tested in a SLA-250 machine using an Ar-ion laser. To determine the SLA parameters, critical exposure (E_c) and penetration depth (D_p), a particular test geometry, called windowpanes[6], was built for each suspension. Each pane in this part receives a different dose and by plotting C_d versus dose, Equation 2 can be utilized to determine D_p and E_c. After prelimary determination of D_p and E_c, three-dimensional parts were fabricated.

Results

Silica

Figure 1 shows the concentration dependence for silica in an aqueous UV-curable solution exposed to the UV lamp radiation[#]. As the volume fraction silica increases the depth of cure decreases in a manner similar to Beer-Lambert behavior with an exponential decay. For volume fractions up to 55 v/o, the suspension's cure depth is above the minimum requirement of 200 μm. Viscosity data will not be shown, but for silica dispersed in the aqueous solutions, the viscosity is below 200 mPa-s for low shear rates, around 3 sec^{-1}, therefore well below the maximum requirement of 3000 mPa-s.

Figure 2 shows the cure behavior for a variety of 50 v/o silica suspensions as a function of exposure dose. As expected, the cure depth increases as the dose increases. However, the larger influence is changing the refractive index of the UV-curable solution. By changing n_o from 1.382 to 1.441, the depth of cure increases from 200 μm to 600 μm at a dose of 1000 mJ/cm^2. A small change in refractive index, about 4%, results in a three-fold increase in cure depth.

Figure 3 shows the first three-dimensional ceramic green body fabricated using stereolithography. The object built is a box, 1" x 1" x 0.75", with a 45 degree angle on one side. This was fabricated from 50 v/o silica dispersed in the aqueous solution having a refractive index of 1.418. The SLA parameters used were D_p= 150 μm and E_c= 80 mJ/cm^2. Each layer is 150 μm thick and 136 layers were built. The approximate build time for this hollow box was about 4 hours.

Figure 4 shows a side view of two boxes built. The sides and the 45 degree angle are built quite accurately, and there was no problem with interlayer adhesion. At the beginning of fabrication, the layers started to curl, most likely due to insufficient supports and the draw style we chose. A raster type draw style was used for the first two parts built and this probably resulted in the curling effect shown in Figure 4. The tops of the boxes are slightly rounded due to the recoat blade was not used during build. The z-wait time was extended to 45 seconds to hopefully allow enough time for the new layer to equilibriate to a flat surface.

Alumina

As shown in Figure 5, the depth of cure is still above the minimum limit of 200 μm for alumina dispersed in the aqueous solution, with the refractive index of 1.418. Moreover, even though the alumina powder has a much smaller particle size, it was easy to maintain a fluid suspension at 50 v/o, with a viscosity of 500 mPa-s at low shear rates.

Figure 6 shows the cure depth versus dose for alumina dispersed in the diacrylate. It is difficult to disperse ceramic powders in non-aqueous solutions, and the maximum solids loading was 40 vol%. For doses larger than 200 mJ/cm^2, the cure depth was greater than

---

[#] It should be noted that the results from the lamp apparatus were not significantly different from the laser results in cure behavior.

200 μm, but the viscosity of the suspension was above 3000 mPa-s. Further rheological studies should help determine the suitable dispersant to maintain a fluid suspension.

Figure 7a shows a representative windowpane for alumina dispersed in the diacrylate. This windowpane was subsequently fired at 1550 °C, resulting in a dense alumina part as shown in Figure 7b.

Theory

The two ceramic materials chosen in this work do not absorb ultraviolet radiation, only scatter the radiation. Light attenuation in a concentrated suspension can be described by the Equation 1. From this equation, there should be three linear relationships: 1) cure depth versus log(E), 2) cure depth versus inverse volume fraction, and 3) cure depth versus inverse of Δn^2. Figure 8 shows the cure depth versus $1/\phi$ for silica and alumina in aqueous solutions. All curves are linear, even at high solids loadings, supporting the scattering equation, Equation 1. Figure 2 showed the cure depth versus dose for a variety of 50 v/o silica suspensions. All curves have linear behavior, further supporting Equation 1.

Lastly, Figure 9 shows the cure depth versus the inverse of Δn^2 for the suspensions of Figure 2. This linear behavior supports that the refractive index difference is the dominating factor controlling the depth of cure. Further theoretical aspects are discussed elsewhere[7].

Conclusions

In summary, the criterion for stereolithography of ceramics have been met: low viscosity and large cure depth for silica and alumina in the aqueous solutions. The cure depth can easily be modified by changing the refractive index.

Three-dimensional parts have been built using a SLA-250 with an Ar-ion laser. Reasonably accurate parts with good interlayer adhesion were built. Further research in the support structure and draw styles should eliminate the curl problems at the beginning of the build.

These first ceramic objects built using stereolithography represent new ways to freeform fabricate ceramic shells and cores, directly, and to fabricate structural ceramic parts.

Acknowledgment

The authors would like to thank Dr. Steve Fishman and Dr. Ralph Wachter at the Office of Naval Research for supporting this work under contract N00014-913-1-0302. We are grateful to Dr. Paul Jacobs, Dr. Thomas Pang, and Kelle Kwo, at 3D Systems, for their time and use of their SLA.

References

1. Pang, T. H. and Jacobs, P. F., "Stereolithography Epoxy Resins SL5170 and SL5180: Accuracy, Dimensional Stability, and Mechanical Properties", Proceedings of the SFF Symposium, Austin, TX, August 8-10, published by the University of Texas at Austin, pp. 204-224, (1994).

2. Krieger, I. M. and Dougherty, T. J., "A Mechanism for Non-Newtonian Flow in Suspensions of Rigid Spheres", Trans. Soc. Rheol. **3**, pp. 137-152, (1959).

3. Jacobs, P. F., Rapid Prototyping and Manufacturing: Fundamentals of Stereolithography, published by the Society of Manufacturing Engineers, Dearborn, MI, pp. 87-94, (1992).

4. Griffith, M. L. and Halloran, "Ultraviolet Curable Ceramic Suspensions for Stereolithography of Ceramics", in Manufacturing Science and Engineering, Vol. 68-2, published by the American Society of Mechanical Engineers, New York, NY, pp. 529-534, (1994).

5. Griffith, M. L. and Halloran, J. W., "Ultraviolet Curing of Highly Loaded Ceramic Suspensions for Stereolithography of Ceramics", Proceedings of the SFF Symposium, Austin, TX, August 8-10, published by the University of Texas at Austin, pp. 396-403, (1994).

6. Jacobs, P. F., Rapid Prototyping and Manufacturing: Fundamentals of Stereolithography, published by the Society of Manufacturing Engineers, Dearborn, MI, pp. 263-281, (1992).

7. Griffith, Michelle, Phd thesis, The University of Michigan, March 1995.

Table 1: Material properties for the ceramic and ultraviolet-curable solutions.

Material	d_{50} (μm)	n
silica	2.29	1.56
alumina	0.34	1.76
aqueous solutions	-	1.382 - 1.441
diacrylate	-	1.457

Table 2: Maximum solids loadings for ceramic suspensions and corresponding viscosities.

Ceramic max v/o	UV-Curable Solution	Viscosity (mPa-s) at 3 sec^{-1}
50 v/o silica	all aqueous solutions 1.382 - 1.441	200 - 500
50 v/o alumina	aqueous 1.382, 1.418	500
40 v/o alumina	diacrylate	> 3000

REPORT DOCUMENTATION PAGE

Form Approved
OMB No. 0704-0188

1. AGENCY USE ONLY (Leave blank)	2. REPORT DATE	3. REPORT TYPE AND DATES COVERED
	August 25, 1997	Final Report 1/1/93 - 12/31/94

4. TITLE AND SUBTITLE

Free Form Fabrication of Ceramics by Stereolithography

5. FUNDING NUMBERS

N00014-93-1-0302

6. AUTHOR(S)

John W. Halloran

7. PERFORMING ORGANIZATION NAME(S) AND ADDRESS(ES)

University of Michigan
Division of Research Development Administration
1058 Wolverine Tower
3003 South State St.
Ann Arbor, MI 48109-1274

8. PERFORMING ORGANIZATION REPORT NUMBER

9. SPONSORING/MONITORING AGENCY NAME(S) AND ADDRESS(ES)

Steven G. Fishman and R. Wachter
Office of Naval Research
800 North Quincy St.
Arlington, VA 22217-5660

10. SPONSORING/MONITORING AGENCY REPORT NUMBER

11. SUPPLEMENTARY NOTES

12a. DISTRIBUTION/AVAILABILITY STATEMENT

Unlimited public availability

12b. DISTRIBUTION CODE

13. ABSTRACT *(Maximum 200 words)*

During this grant we showed that stereolithography can directly fabricate ceramic green bodies from ultraviolet (UV) curable solutions which contain dispersed ceramic powders. We demonstrated SLA of silica, a model refractory for metal casting molds, and SLA of alumina, which is promising for structural ceramics. Viscosity control for these highly concentrated suspensions and cure depth behavior were the main issues for fabricating a ceramic using stereolithography techniques. These ceramic SLA suspensions were evaluated in a stereolithography machine, and three-dimensional parts were built. Part building parameters, D_p and E_c were determined for this suspension. Layer adhesion and subsequent processing resulted in good ceramic parts.

14. SUBJECT TERMS

solid freeform fabrication, rapid prototyping, ceramics, stereolithography

15. NUMBER OF PAGES

9

16. PRICE CODE

17. SECURITY CLASSIFICATION OF REPORT	18. SECURITY CLASSIFICATION OF THIS PAGE	19. SECURITY CLASSIFICATION OF ABSTRACT	20. LIMITATION OF ABSTRACT
unclassified	unclassified	unclassified	unlimited

GENERAL INSTRUCTIONS FOR COMPLETING SF 298

The Report Documentation Page (RDP) is used in announcing and cataloging reports. It is important that this information be consistent with the rest of the report, particularly the cover and title page. Instructions for filling in each block of the form follow. It is important to ***stay within the lines*** to meet ***optical scanning requirements***.

Block 1. Agency Use Only *(Leave blank)*.

Block 2. Report Date. Full publication date including day, month, and year, if available (e.g. 1 Jan 88). Must cite at least the year.

Block 3. Type of Report and Dates Covered. State whether report is interim, final, etc. If applicable, enter inclusive report dates (e.g. 10 Jun 87 - 30 Jun 88).

Block 4. Title and Subtitle. A title is taken from the part of the report that provides the most meaningful and complete information. When a report is prepared in more than one volume, repeat the primary title, add volume number, and include subtitle for the specific volume. On classified documents enter the title classification in parentheses.

Block 5. Funding Numbers. To include contract and grant numbers; may include program element number(s), project number(s), task number(s), and work unit number(s). Use the following labels:

C	- Contract	**PR**	- Project
G	- Grant	**TA**	- Task
PE	- Program Element	**WU**	- Work Unit Accession No.

Block 6. Author(s). Name(s) of person(s) responsible for writing the report, performing the research, or credited with the content of the report. If editor or compiler, this should follow the name(s).

Block 7. Performing Organization Name(s) and Address(es). Self-explanatory.

Block 8. Performing Organization Report Number. Enter the unique alphanumeric report number(s) assigned by the organization performing the report.

Block 9. Sponsoring/Monitoring Agency Name(s) and Address(es). Self-explanatory.

Block 10. Sponsoring/Monitoring Agency Report Number. *(If known)*

Block 11. Supplementary Notes. Enter information not included elsewhere such as: Prepared in cooperation with...; Trans. of...; To be published in.... When a report is revised, include a statement whether the new report supersedes or supplements the older report.

Block 12a. Distribution/Availability Statement. Denotes public availability or limitations. Cite any availability to the public. Enter additional limitations or special markings in all capitals (e.g. NOFORN, REL, ITAR).

- **DOD** - See DoDD 5230.24, "Distribution Statements on Technical Documents."
- **DOE** - See authorities.
- **NASA** - See Handbook NHB 2200.2.
- **NTIS** - Leave blank.

Block 12b. Distribution Code.

- **DOD** - Leave blank.
- **DOE** - Enter DOE distribution categories from the Standard Distribution for Unclassified Scientific and Technical Reports.
- **NASA** - Leave blank.
- **NTIS** - Leave blank.

Block 13. Abstract. Include a brief *(Maximum 200 words)* factual summary of the most significant information contained in the report.

Block 14. Subject Terms. Keywords or phrases identifying major subjects in the report.

Block 15. Number of Pages. Enter the total number of pages.

Block 16. Price Code. Enter appropriate price code *(NTIS only)*.

Blocks 17. - 19. Security Classifications. Self-explanatory. Enter U.S. Security Classification in accordance with U.S. Security Regulations (i.e., UNCLASSIFIED). If form contains classified information, stamp classification on the top and bottom of the page.

Block 20. Limitation of Abstract. This block must be completed to assign a limitation to the abstract. Enter either UL (unlimited) or SAR (same as report). An entry in this block is necessary if the abstract is to be limited. If blank, the abstract is assumed to be unlimited.